2020

Protein Encapsulation Using Complex Coacervates: What Nature Has to Teach Us

Whitney C. Blocher McTigue

Sarah L. Perry

Protein Encapsulation using Complex Coacervates: What Nature has to Teach Us

Whitney C. Blocher McTigue and Sarah L. Perry*
Department of Chemical Engineering, University of Massachusetts Amherst
*Correspondence: perrys@engin.umass.edu

Abstract

Protein encapsulation is a growing area of interest, particularly in the fields of food science and medicine. The sequestration of protein cargoes has been achieved using a variety of methods, each with benefits and drawbacks. One of the most significant challenges associated with protein encapsulation has been achieving high loading while maintaining protein viability. This difficulty has been exacerbated because many encapsulant systems require the use of organic solvents. In contrast, nature has optimized strategies to compartmentalize and protect proteins inside the cell – a purely aqueous environment. Although the mechanisms whereby aspects of the cytosol is able to stabilize proteins are unknown, the crowded nature of many newly discovered, liquid phase separated 'membraneless organelles' that achieve protein compartmentalization suggests that the material environment surrounding the protein may be critical in determining stability. Here, we focus on encapsulation strategies based on liquid-liquid phase separation, and complex coacervation in particular, which has many of the key features of the cytoplasm as a material. We review the literature on protein encapsulation via coacervation and discuss the parameters relevant to creating protein-containing coacervate formulations. Additionally, we highlight potential opportunities associated with the creation of tailored materials to better facilitate protein encapsulation and stabilization.

Introduction

Most formulations of proteins, whether for laboratory use or for applications such as biocatalysis or medicine, could likely be described as relatively dilute in the protein of interest,[1,2] and have a dramatically different material context compared with the natural intracellular environment. In the cell, despite close interactions with a range of other biomacromolecules (*i.e.*, the cytosol is ~30% protein by mass),[3-5] proteins remain in their folded native state. This difference in environment may explain why proteins are stable in the body, but not as kinetically stable (in terms of shelf life) in formulations. Even under optimal solution conditions, this storage stability varies widely and often still requires refrigeration.[6,7] While a number of parallels can be drawn directly between strategies for encapsulation and naturally occurring features in cells,[8-12] efforts to date have largely focused on compartmentalization to protect protein cargo from degradation due to *external* factors rather than formulation to enhance the stability of the protein itself.

As research to develop new strategies for protein encapsulation and delivery has accelerated in recent years, there have been a number of separate and unrelated efforts to understand the ways in which cells are able to selectively compartmentalize and store proteins.[13,14] In particular, there has been tremendous excitement surrounding the discovery of liquid-liquid phase separation as a mechanism for localizing specific proteins, RNA, and other biomolecules.[15-17] Many of these liquid granules (also termed 'membraneless organelles' and 'biomolecular condensates')[18] have been shown to act as a locus for specific catalytic reactions, or as a compartment to store specific enzymes during times of stress.[19-23] Phase separation enables preferential partitioning of specific molecules, as well as the potential stabilization of guest proteins by modulating the material context of the environment. Furthermore, liquid-liquid phase separation enables preferential compartmentalization while avoiding the challenges of an impermeable boundary, such as a lipid bilayer.

Here, we will briefly review a range of different encapsulation strategies used for the separation, purification, and delivery of proteins, before focusing more specifically on the use of liquid-liquid phase separation, and particularly complex coacervation for these applications. We will discuss the formulation of coacervate-based materials, including strategies for achieving efficient uptake of proteins. We will also discuss experimental strategies for characterizing the uptake of proteins into coacervate-based formulations, and how these types of complex formulations might better imitate the natural intracellular environment to improve protein stability.

The Challenge of Protein Encapsulation

A wide variety of methods have been described in the literature for the encapsulation of proteins. These strategies have included oil-and-water emulsions, physical and/or chemical entrapment in solid nano- or microparticle systems, engulfment into liposomes/vesicles/polymerosomes, and partitioning or entrapment into phase separated materials such as polymer microparticles, nano- or microgels, segregative aqueous two-phase systems (ATPS), and associative complex coacervates (Figure 1).[24-27] However, a majority of these methods that do not use ATPS, particularly liposomes, gels, and particle systems, tend to suffer from low loading efficiencies and typically require the use of organic solvents that may destabilize the protein cargo. We will briefly introduce disadvantages that can be overcome using complex coacervation with these methods below, but refer the reader to the listed references for a more complete discussion.

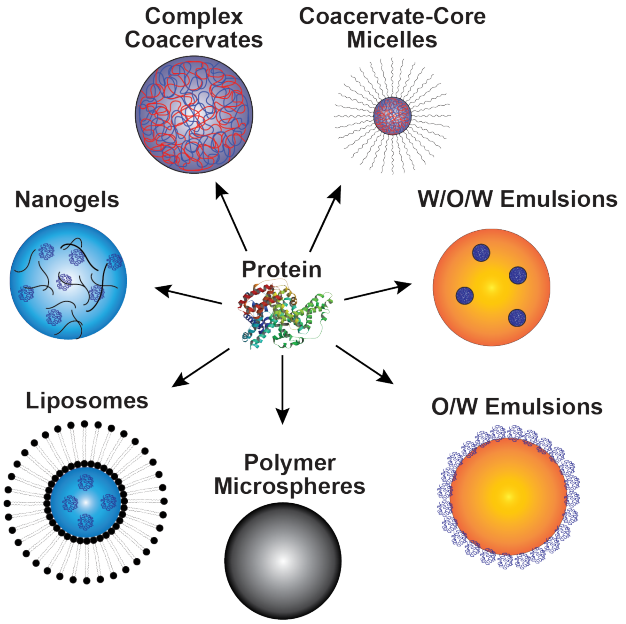

Figure 1. Different encapsulation methods for proteins. From the top, moving clockwise: complex coacervates, coacervate-core micelles, water-in-oil-in-water (W/O/W) emulsions, oil-in-water (O/W) emulsions, polymer microspheres, liposomes, and nanogels.

Two main concerns for many of the protein encapsulation methods are: use of organic solvents, and the low protein encapsulation efficiencies and loading. For example, emulsion and nanogel methods utilize the immiscibility of oil and water phases to achieve compartmentalization. Proteins would generally be prepared in an oil or aqueous solution for emulsification, depending on their solubility, and then mixed with an aqueous or organic phase, respectively, to achieve compartmentalization.[24,25,28-30] Similarly, many of the methods to prepare polymer microspheres also utilize organic solvents.[31] The most prominent utilize emulsions techniques or solvent extraction with polymers such as poly(lactic acid) and poly(lactic-co-glycolic acid).[31,32] Although protein encapsulation efficiency can be tuned with polymer microspheres, the use of organic solvents can lead to protein denaturation. Proteins encapsulated by these types of methods are vulnerable to aggregation, denaturation, and cleavage,[33] particularly at the interface between aqueous and organic solvent phases.

Additionally, many of these techniques can suffer from low encapsulation efficiencies and loadings. Vesicular structures such as liposomes and polymersomes take inspiration from the lipid bilayers that define cells. These structures are created using amphiphilic lipids or polymers to create a bilayer structure that can encapsulate hydrophilic substances within the aqueous lumen and amphiphilic or lipophilic substances within the bilayer shell.[24,34,35] However, because these types of structures rely on engulfment of an aqueous phase, these systems tend to have very low encapsulation efficiencies (*i.e.*, mass recovery of protein). The limitations of engulfment can be overcome through the use of droplet microfluidics, where oil-in-oil and water-in-oil techniques can be used to generate vesicular structures with near 100% encapsulation efficiency.[36-38] Additionally, as with emulsion strategies, the overall level protein loading is limited by the concentration of the aqueous phase that can be used during formulation.

The concept of physical partitioning of cargo has commonly been used in systems that undergo macroscale aqueous two-phase separation (ATPS). This type of phase behavior could be the result of segregative phase separation (*e.g.*, poly(ethylene glycol) (PEG)/dextran),[39-41] polymers that undergo either a lower critical solution temperature (LCST) or an upper critical solution temperature (UCST) transition based on interactions with water,[42] such as elastin-like polypeptides (ELPs),[43,44] or complex coacervates that form due to associative interactions between polymers. These types of materials have the advantage of allowing for fully-aqueous processing, and have been used broadly for protein purification, with coacervates finding particular utility in delivery.[45-50] Furthermore, the phase-separated nature of these materials allows for strong partitioning of proteins into the polymeric phase, allowing for

the easy preparation formulations with a high encapsulation and/or loading of protein. [12,51-53] These high levels of incorporation are mainly due to the electrostatics and entropic gains associated with phase separation, but also take advantage of differences in the overall polarity of the coacervate environment compared to pure water.[54-57] To the best of our knowledge, there are only a few instances of ELPs and PEG/dextran delivery systems reported in the literature.[58-60] Here we will focus on complex coacervation as a platform for protein encapsulation.

Complex Coacervation, Phase Behavior, and Biomimicry

Complex coacervation, [49,51,52,56,57,61-73] whose characteristics mimic the characteristics of cells, is a simple, purely aqueous strategy for encapsulating proteins. Complex coacervation is a liquid-liquid phase separation phenomenon resulting from the association of two oppositely charged macro-ions (*e.g.*, polymer, protein, surfactant micelles). Coacervation results in the formation of a dense, macromolecule rich coacervate phase in equilibrium with a macromolecule-poor supernatant (Figure 2).[52,74-84] The coacervate phase retains both water and salt in addition to the polyelectrolytes, with typical compositions ranging between 65 and 85% water.[85-88] This phase separation is highly dependent on the relative amount and identity of the polyelectrolytes present, as well as pH, ionic strength, ion identity, temperature, and other such factors.[76,80,81,83,87,89-93]

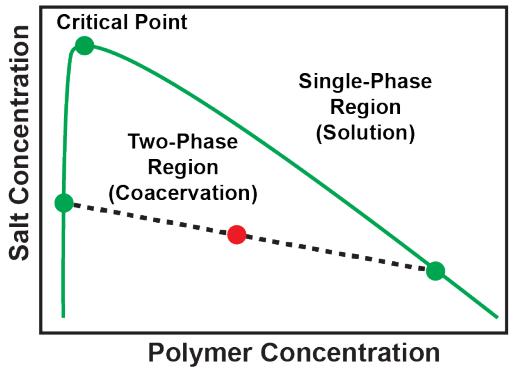

Figure 2. Generic depiction of a coacervation phase diagram showing the binodal phase boundary as a function of salt and polymer concentration at a specified polymer charge ratio, pH, and temperature. Samples prepared in the two-phase region beneath the binodal curve (red dot) will phase separate into the polymer-poor supernatant and polymer-rich coacervate phases along a tie-line (dashed line). Above the binodal curve is the single-phase region where no phase separation is observed.

If we think of the width of the two-phase region as an indicator of the stability of the coacervate, various factors such as the stoichiometry, pH, salt, and temperature, as well as the length and patterning of charges along the polyelectrolytes selected, and the chemistry of the polyelectrolytes can affect the phase behavior. Increasing the length of the polyelectrolytes used will increase the width of the two-phase region,[51,81,83,94,95] as will increasing the polymer charge density,[96,97] and/or the blockiness of charged segments.[95,98-100] Additionally, increasing the hydrophobicity of a polymer,[101,102] the polarity,[103] and/or incorporating orthogonal associative interactions (*e.g.*, hydrogen bonding,[74,104,105] cation-π interactions,[106] etc.) can also stabilize the coacervate, although these effects are more complex to predict.

The Effect of Charge Stoichiometry and Ionic Strength

While the vast chemical diversity of polymers, proteins, and other macro-ions creates a near infinite number of possible interactions to consider, the majority of coacervate experiments focus on two parameters, charge stoichiometry and ionic strength. For the simple case of two oppositely-charged polymers, maximum coacervation will be achieved under conditions where an equal number of positive and negatively charged polymer groups are present. Shifting the charge stoichiometry of the mixture, either by changing the composition or altering the solution pH will lead to an excess of one of the species,

and thus a smaller number of complexing chains. Phenomenologically, these trends are commonly observed via turbidity measurements, either as a function of the fraction of one of the charged species present, or as a function of pH (Figure 3).[76,107] However, it is important to note that turbidity is only a measure of the amount of surface area present in the sample. Thus, a higher turbidity signal could correlate with more smaller droplets or fewer larger droplets, and care should be taken not to over-interpret such data.

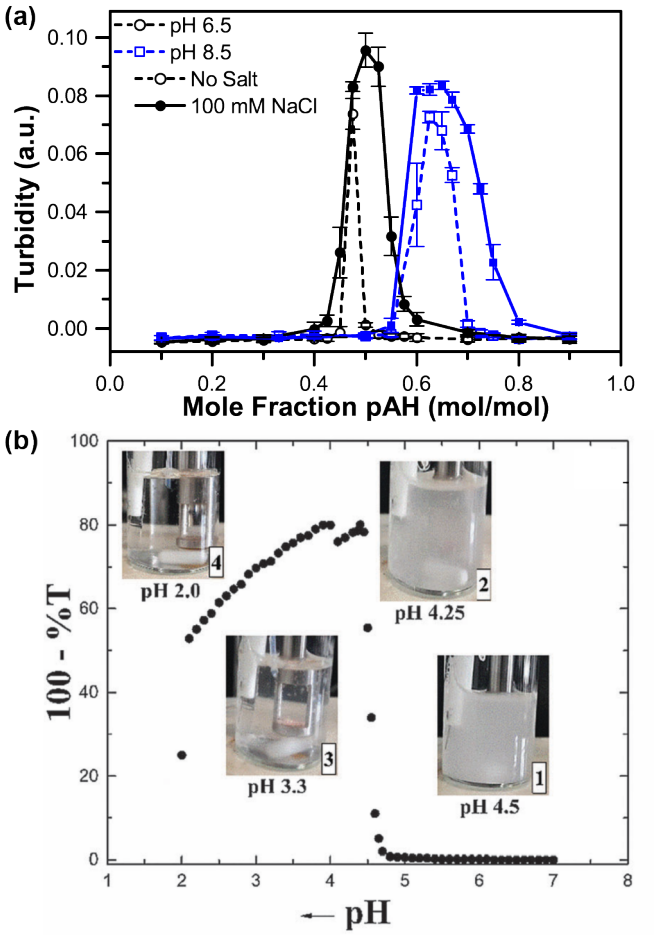

Figure 3. (a) A plot of turbidity as a function of the charge fraction of the polycation at pH 6.5 and 8.5. All samples were prepared at 1 mM total monomer concentration, 50/50 mol% poly(acrylic acid sodium salt) (pAA)/poly(allylamine hydrochloride) (pAH). Complexes were prepared by adding pAA to a solution containing pAH. (Reprinted with permission from Ref. 76. Copyright 2014 Open Access from Polymers.) **(b)** pH dependence of the turbidity and system state for hyaluronic acid (0.1 g/L) and β-lactoglobulin (1 g/L) mixture with respect to pH in 25 mM NaCl, upon addition of acid. (Reproduced from Ref. 107, with permission from The Royal Society of Chemistry.)

While nearly all of the parameters that we have discussed thus far with respect to coacervate stability can be explained using our intuition of electrostatics, the effects of salt are often the easiest to misinterpret. The addition of salt has been shown to weaken the electrostatic interactions between complexing macro-ions. In this sense, ionic strength plays a role similar to that of temperature. Thus, it would be easy to assume that the addition of salt merely "screens" the electrostatic interactions between the two polymers. While the effects of charge screening may be true for coacervate systems that destabilize in the range of physiological levels of saline, where the Debye length approaches the length scale of atoms (Figure 4a), there are a significant number of example systems which show salt resistance up to several molars of salt (Figure 4b). Thus, while electrostatic interactions are behind many of the

interactions driving coacervation, the energetic driving force ultimately comes from the large amount of entropy gained by the release of small counterions when two oppositely-charged polyelectrolytes form a complex. Therefore, the concentration of salt above which phase separation is no longer observed (*i.e.*, the salt resistance) corresponds to the point where the concentration of ions in solution has disfavored the entropic release of those counterions localized around the polymers. In addition to valence, the identity of the salt can also have a dramatic effect on coacervate stability. To a first approximation, the trends in salt resistance scale with ionic strength.[76] However, important secondary effects related to the interaction of the salt ions with water can also be very significant (Figure 4b).

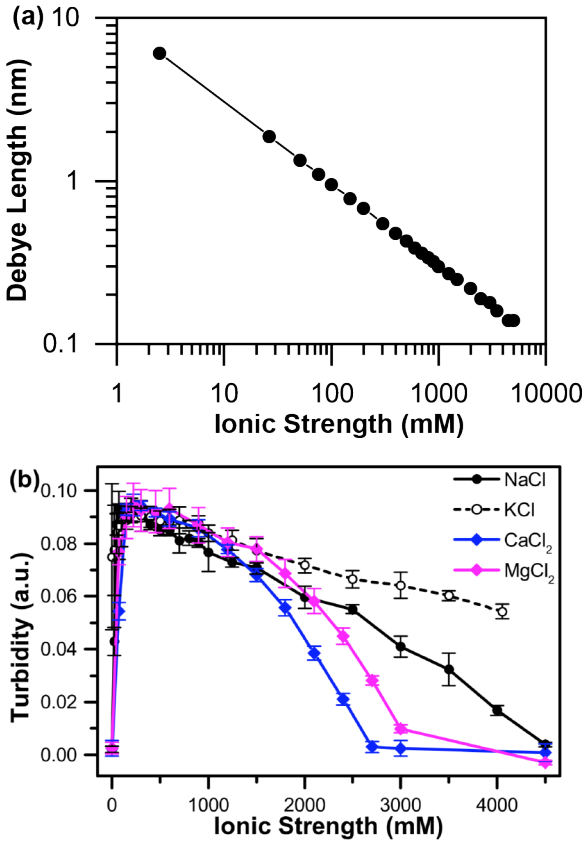

Figure 4. (a) Calculated values of the Debye length as a function of ionic strength. **(b)** A plot of turbidity as a function of ionic strength for a series of chloride salts, investigating the effects of various cations. All samples were prepared at 1 mM total monomer concentration, 50/50 mol% poly(acrylic acid sodium salt) (pAA)/poly(allylamine hydrochloride) (pAH) ratio at pH 6.5. Complexes were prepared by adding pAA to a solution containing a mixture of pAH and the desired quantity of salt. (Reprinted with permission from Ref. 76. Copyright 2014 Open Access from Polymers.)

Charge Patterning

As we look to push our understanding of complex coacervation towards more bioinspired materials based on the intrinsically disordered proteins (IDPs) that form liquid-liquid phase separated granules in cells, chemical sequence becomes a critical parameter. Recent studies by Perry and Sing and coworkers using sequence-controlled polypeptides have elucidated the way in which patterns of charge affect coacervate phase behavior (Figure 5).[95,98-100,108,109] Intuition might have suggested that the most important factor dictating phase behavior would be matching of charge sequence (*i.e.*, optimization of the attractive electrostatic interactions between the two polymers). However, experimental and computational results highlighted the critical role of charge sequence in structuring counterions along each individual polyelectrolyte *before* complexation takes place. Consider sequence-controlled polymers with a regular

pattern of charged and neutral monomers in solution. While oppositely-charged counterions will tend to localize around a polymer to neutralize its charge, the effect of sequence can be dramatic. For a polymer with a relatively small charged block, there is little electrostatic difference for the counterion to localize directly on a charged monomer vs. on a neighboring residue. However, for the case of a very blocky structure, there would be a tremendous electrostatic penalty for counterions to localize in the middle of a neutral block (Figure 5d). In this way, the sequence of the polymer dictates the entropic benefit gained from the release of these small counterions upon complexation by determining their initial state. Similar effects were also observed for the self-coacervation of polyampholytes composed of patterns of positive and negative charges.[95] However, in this case the entropic effects of counterion clustering are further convoluted by the presence of charge-sign interfaces where neighboring oppositely-charged monomers are able to self-neutralize and obviate the need for condensed counterions (Figure 5e).

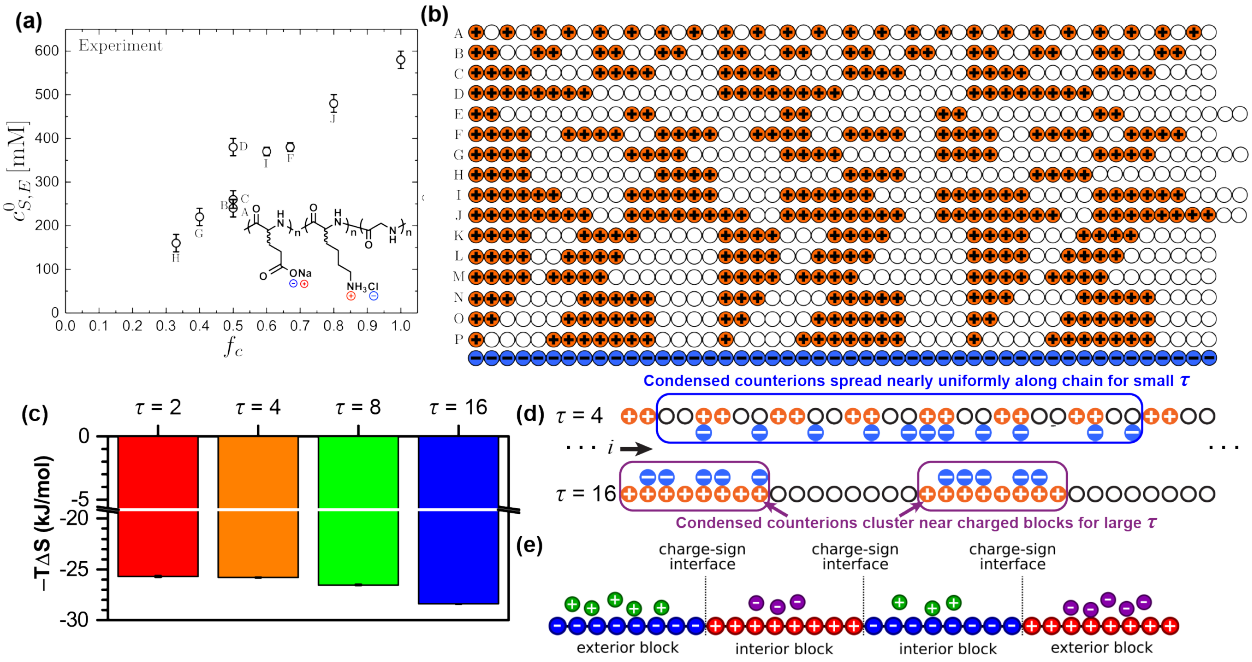

Figure 5. (a) Plot of salt resistance vs. charge fraction using poly(glutamate) with patterned cationic poly(lysine-co-glycine), as described in **(b)**. (Reprinted with permission from Ref. 99. Copyright 2019 Open Access from ACS Central Science.) **(c)** Entropic gains as a function of charged block size determined using isothermal titration calorimetry. Schematic depiction of the differences in counterion localization for different patterns of charge for **(d)** polyelectrolytes (Reprinted with permission from Ref. 98. Copyright 2017 Open Access from Nature Communications.) and **(e)** polyampholytes. (Ref. 95, Madinya, *et al.*, Sequence-dependent self-coacervation in high charge-density polyampholytes. *Mol. Syst. Des. Eng.* **2020**, Advance Article , DOI: 10.1039/C9ME00074G - Reproduced by permission of The Royal Society of Chemistry.)

Hierarchical Structure

While the results to date have focused on complex coacervates that undergo macrophase separation, it is also possible to take advantage of block copolymer architectures to facilitate hierarchical microphase separation. In particular, a majority of efforts have coupled a water soluble polymer block, such as poly(ethylene glycol) (PEG)[69,110] or poly(oligoethylene glycol methacrylate) (POEGMA)[91] to one or both of the oppositely-charged polymers. This block copolymer structure creates an interface that drives microphase separation, with the relative length of the two blocks dictating the resulting structure. Generally speaking, a longer hydrophilic polymer block will lead to the formation of spherical coacervate- or polyion complex core micelles (CCMs or PIC micelles) typically in the range of ~30 nm in diameter,[68,111,112] while a shorter hydrophilic block will allow for the formation of lower curvature

structures, such as polyion-complex vesicles, or PICsomes that can be significantly larger (Figure 6).[61,113-116] The size of CCMs, however, can be larger with the inclusion of cargo.[64,67,91] While more complex morphologies, including coacervate-corona micelles, cross-linked hydrogels, arrays of spheres, and hexagonal rods can also be formed, they are beyond the scope of the current review.[117-122]

Generally speaking, the same design rules apply in terms of charge stoichiometry, pH, etc. for these hierarchical coacervate-based structures as for bulk materials, although the overall stability tends to be slightly lower due to the added constraint of the interface.[91] However, the true utility of micellar or vesicular structures comes in the context of stable formulations, particularly for delivery. Bulk coacervates have the tendency to coalesce over time, forming a bulk coacervate liquid, rather than a dispersion of droplets.[123,124] In contrast, micelles allow for encapsulation of cargo in the coacervate core, while the presence of the neutral polymer corona prevents coalescence and can facilitate stealth properties for intravenous delivery applications.[47,64,67,68,125,126]

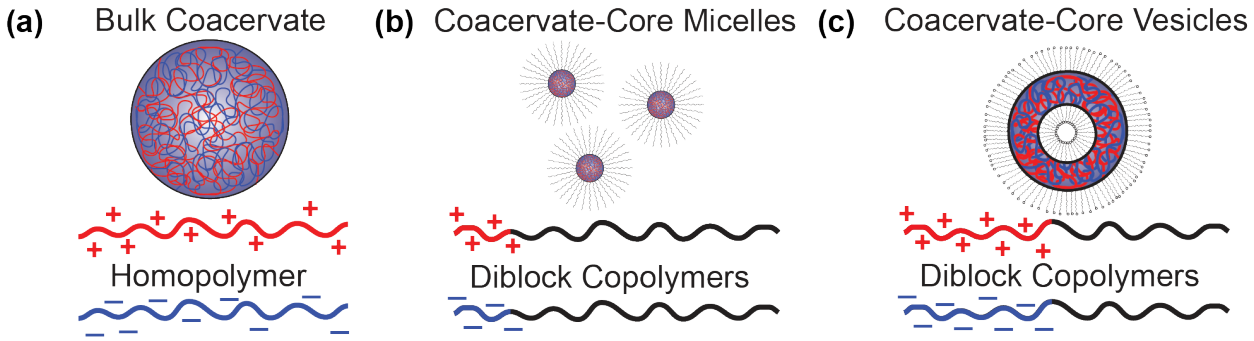

Figure 6. Representations of **(a)** bulk coacervates, **(b)** coacervate-core micelles (CCMs or PIC micelles), and **(c)** coacervate-core vesicles (PICsomes). Bulk coacervates typically utilize homopolymers or random copolymers, while coacervate-core micelles and vesicles more typically use diblock copolymers.

While the general trends described thus far provide a useful guide to understanding of the phase behavior of coacervate-based materials, this intuition does not necessarily extend to cases where proteins are involved. In these cases, the more complex chemical nature of proteins can lead to seemingly incongruent results that require molecular-level inspection to understand.

Complex Coacervates Incorporating Proteins

A variety of different types of complex coacervate-based strategies have been studied and used for the incorporation and/or encapsulation of proteins. Coacervation has the benefit of purely aqueous processing and has the ability to achieve high concentrations of the cargo molecule of interest. The application for such protein-containing materials has dictated the type of coacervate architecture, the selection of polyelectrolytes, and the environmental factors of the system.

Electrostatics: The Role of Protein Charge

Complex coacervation is highly dependent on electrostatics as a driving force to achieve net neutrality. This is both fortuitous and a drawback. Proteins are made up of diverse amino acids, specifically those that are neutral, negatively charged and positively charged. Thus, these biomacromolecules are almost always charged in some capacity with respect to pH, though they may not have a net charge. However, this electrostatic nature in and of itself does not differentiate between charged species, so multiple cargoes may be encapsulated at once if each species has sufficient charge. We will discuss the possibility of modulating protein charge to enable purification later on.

Much of the early work involving coacervation focused on the formation of these materials from milk-derived proteins for applications in the food industry.[127-129] Here, the goal was not necessarily the encapsulation or stabilization of a specific enzyme, but the creation of protein and/or polysaccharide dispersions for the modification of food texture and/or the delivery of flavor additives, nutraceuticals,

etc.[130-133] In these studies, because the role of the protein was more structural, studies typically focused on the effect of pH and/or temperature to drive phase separation (see Figure 3b). Thus, various combinations of proteins and/or polysaccharides could be chosen to fit the application of interest.

These studies on protein-based complex coacervates emphasized the importance of solution pH as a strategy for controlling the net charge of the various species present. Thus, the solution pH could generally be compared with the isoelectric point (*i.e.*, the pI defines the solution pH at which the *net* charge of a protein is zero, not that no charges are present) to predict conditions where coacervation would occur. The pI of a protein can be estimated theoretically through the Henderson-Hasselbalch equation, and has been incorporated into a range of online tools such as ProtParam,[134] or can be determined experimentally via titration. At solution pH conditions below the pI, a protein carries a net-positive charge, while above the pI the protein is net negative (Figures 10a,d). However, a series of reports highlighted instances where coacervation was observed "on the wrong side of the pI."[135-148] These studies determined that this unintuitive result was a consequence of charge anisotropy, or clustering of charges on the globular proteins. Thus, as in the case of charge patterning on linear polymers,[95,98,99] the clustering of charges can lead to entropic counterion condensation/release effects that can dominate over "pure" electrostatic interactions, dictated by the net protein charge.

In an attempt to better quantify the importance of protein charge on the ability of a protein to undergo complex coacervation with an oppositely-charged polymer, Obermeyer and co-workers took advantage of both chemical ligation and mutagenesis strategies to create "supercharged" proteins. This approach allowed for modification of the charged state of a single protein without changing its overall structure, thus avoiding the complication of trying to compare results from different proteins. Obermeyer *et al.*, demonstrated that a threshold level of net charge is needed to enable coacervation of anionic proteins with a strong cationic polymer.[11,12,91] To observe complex coacervation, a charge ratio (*i.e.*, number of negative charges to positive charges on the protein) greater than 1.1 – 1.2 was required (Figure 7).[91] While methods such as chemical ligation or point mutations could be used to modify the net charge of a protein without altering solution conditions, there are numerous targets that might be inaccessible to such an approach.

In a later report, Obermeyer and co-workers explored the potential of adding a charged protein tag to onto globular proteins to promote liquid-liquid phase separation.[12] Their report, which used green fluorescent protein (GFP) as a model system, demonstrated that the presence of a terminal sequence of charged residues was able to drive phase separation when the same protein with an isotropic distribution of charges was not observed to coacervate. Thus, the addition of a terminal ionic tag could be used to facilitate phase separation for reasons of purification as well as formulation.

While bulk phase separation allows for the straightforward characterization of protein-polyelectrolyte complex coacervates, different morphologies, such as CCMs, allow for control of the final complex size and avoid the issue of droplet coalescence. Several reports have focused on the use of a target protein and an oppositely-charged polyelectrolyte to form CCMs.[64,91,110,149,150] The CCM size in these systems were shown to be tunable based on protein and solution conditions, such as solvent and salt concentration.[64,91,110,149] However, because of the geometric constraints of the micelle, the stability of a micellar system was typically somewhat lower than the equivalent macrophase separated system.[91] Interestingly, work by Harada and Kataoka incorporating lysozyme into CCMs via complexation with a poly(ethylene glycol)-*b*-poly(aspartate) showed an enhancement in enzyme activity upon incorporation,[151] supporting the idea of using the material environment to enhance protein activity.

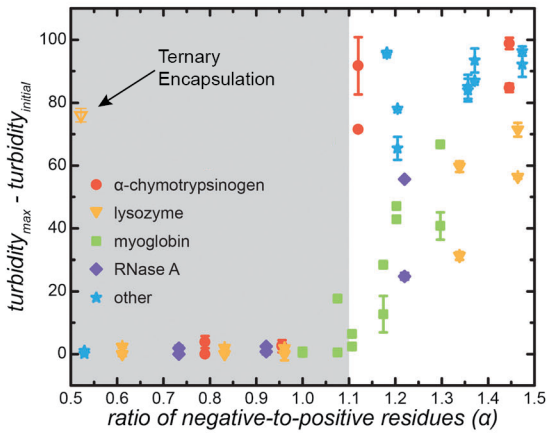

Figure 7. Identification of predictive parameters for globular protein coacervation. Plot of changes in turbidity as a function of the ratio of negative-to-positive residues on the protein. Variation in charge ratio was achieved by acetylation of protein surface residues. The grey shaded region corresponds to proteins that do not phase separate (α < 1.1). The other proteins tested include: trypsin, α-amylase, β-lactoglobulin, bovine serum albumin, cytochrome $P450_{BM3}$, and mCherry. Open triangle data from Blocher McTigue and Perry for lysozyme in a ternary system.[51] (Reprinted and adapted with permission from Ref. 91. Copyright 2016 Soft Matter.)

For applications where high loadings of protein in the coacervate are desired, pairing a protein with a single, oppositely-charged polymer would be expected to lead to the most efficient formulation (*i.e.*, highest per mass incorporation of protein). However, the complexity of proteins and enzymes is such that the solution conditions that might be optimal for coacervation might not be favorable for activity or stability. However, naturally occurring membraneless organelles in cells,[8,18,42,152-160] which are typically formed from a mixture of intrinsically disordered proteins and RNA, indicate that a multi-component system may be more amenable to the incorporation of specific globular proteins without the need for external pH control. Some of these membraneless organelles have been shown to form via complex coacervation.[15-17]

Work by Tirrell and co-workers, demonstrated the ability to achieve high levels of protein incorporation through the use of a ternary system where the protein of interest is complexed with a mixture of cationic and anionic polymers (Figure 8).[52] Additionally, work by the same group showed that complexation over a broader range of polymer compositions than would be expected with traditional binary systems by using coacervates formed from a ternary system.[77] Further experiments by multiple groups explored the potential of this approach for the encapsulation various polymer/protein systems.[3,10,24,33,51,56,57,110,161]

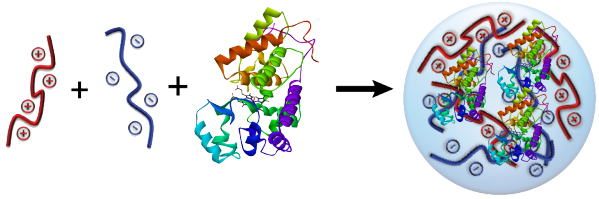

Figure 8. Schematic depiction of complex coacervation in a ternary system with two oppositely charged polyelectrolytes and a protein of interest.

While two-polymer coacervate systems have been shown to enable the incorporation of weakly charged proteins, optimization of coacervation parameters remains critical for efficient protein incorporation. For the case of charge stoichiometry, the introduction of a protein as a third charged species complicates the formulation of design rules. The coacervate system will always reach a charge

neutral composition, but the large differences in charge content and charge density between the polymers and a guest protein can lead to competitive interactions between the various species.[162] The effect of this competition can be observed by comparing results for the incorporation of a cationic protein lysozyme into two different coacervate systems (Figure 9). In recent work by Blocher McTigue and Perry, the effect of charge stoichiometry on protein incorporation was tested at conditions of constant total polymer concentration while varying the relative amount of polycation to polyanion.[51] The results of this experiment showed only a slight shift in the optimum 1:1 ratio of polyanion and polycation, commensurate with the presence of a small amount of a cationic protein (Figure 9a). In contrast, work by Lindhoud and co-workers determined an optimum polymer ratio by holding the amount of the protein and polyanion constant and varying the concentration of the polycation.[10,57] Their results also showed a shift in the optimum charge stoichiometry towards net negative conditions, albeit a much more dramatic one (Figure 9b). While the difference in these results is subtle, and could be attributable to parameters such as differences in protein concentration or the various polymer systems used, Lindhoud and co-workers also reported results for the incorporation of succinylated lysozyme as an equal and oppositely-charged model for comparison (Figure 9b). Interestingly, the optimum condition for the negatively-charged succinylated lysozyme did not occur at the net positive charge stoichiometry that intuition would predict. This combination of results highlights the need for more in-depth studies of the effect of varying all three components (polycation, polyanion, and protein), as well as the net charge and charge distribution on the protein in order to establish design rules guiding protein incorporation.

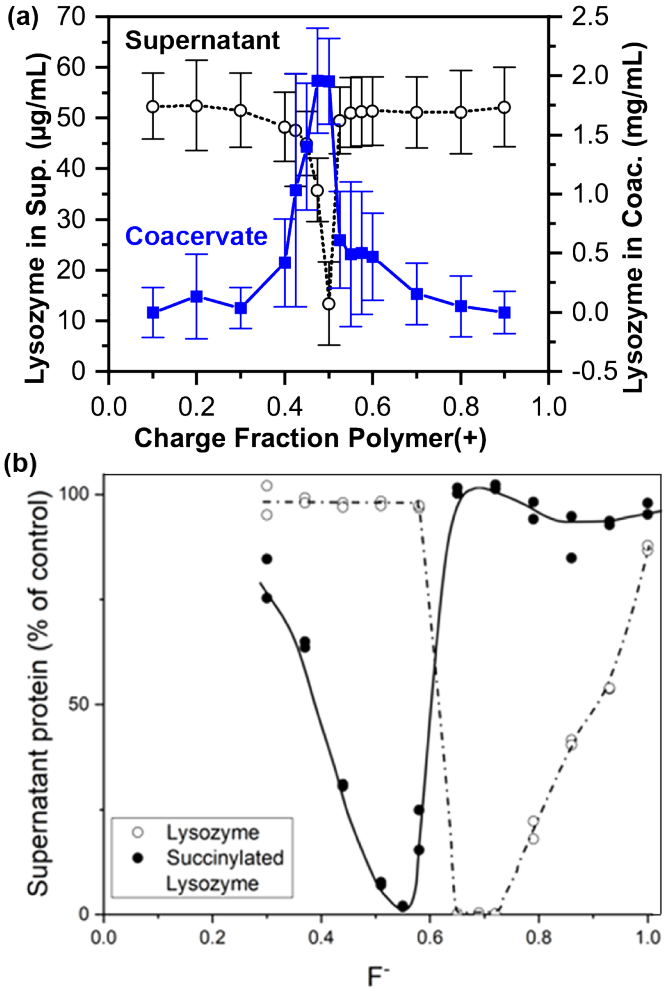

Figure 9. (a) Plot of the concentration of hen egg white lysozyme in the supernatant (dashed black) and coacervate (solid blue) as a function of the charge fraction of the polycation. (Ref. 51, Blocher McTigue and Perry, Design Rules for Encapsulating

Proteins into Complex Coacervates. *Soft Matter* **2019**, *15*, 3089–3103 – Reproduced by permission of The Royal Society of Chemistry.) **(b)** Plot of the concentration of protein in the supernatant (expressed as a percentage of the control system without polyelectrolytes) as a function of the charge fraction of the polyanion f^- for positively-charged lysozyme (net charge of +7) and anionic lysozyme created by succinylation (net charge of -7) in complex with poly(acrylic acid) (PAA) and poly(allylamine hydrochloride) (PAH) at pH in the range of 7.0 – 7.4. The optimum values of f^- for each protein can be identified from the minima on the graph. f_{opt}^- = 0.65 for lysozyme and f_{opt}^- = 0.55 for succinylated lysozyme. (Reprinted with permission from Ref. 10. Copyright 2019 Open Access from Biomacromolecules.)

Beyond the challenge of charge stoichiometry, other parameters such as solution pH, ionic strength, and the charge density of the complexing polymers can also play a key role. As might be expected based on intuition, changing the solution pH to modulate the net charge on the protein (assuming no significant change in the charge state of the two polymers) can dramatically affect the level of protein incorporation.[51,142] For proteins such as bovine serum albumin (BSA) that have an acidic pI, increasing the solution pH allows the protein to become more negatively charged, and increases protein uptake (Figure 10b). Conversely, a protein like lysozyme that has a basic pI will become more positively charged at lower pH (Figure 10e).

Despite the similarity in the trends of increasing protein encapsulation with changes in pH away from the pI, these two proteins show dramatically different levels of uptake. The authors hypothesized that the relatively low levels of BSA incorporation were a consequence of the relatively isotropic distribution of charges on the surface of the protein (Figure 10a), while the uptake of lysozyme was enhanced by the presence of a cluster of cationic residues (Figure 10d).[51] While this information is useful from a formulation standpoint, it also highlights the original function of these two proteins. As a serum protein, BSA has likely evolved to present a surface that does not favor binding or aggregation. In contrast, the charge patch on lysozyme is involved in substrate binding.[163-165] Thus, the molecular level features that help to define protein function may also help to inform the formulation of systems for encapsulation and potentially stabilization.

As in the case of simple two-polymer coacervates, increasing the ionic strength of the system will serve to weaken the electrostatic interactions and disfavor the entropic driving force for coacervate formation. However, for the case of complex coacervates formed from two polymers as well as a protein, the addition of salt will first disfavor complexation of the most-weakly charged species. Thus, increasing ionic strength can decrease or even eliminate the incorporation of protein into the coacervate before phase separation itself is eliminated.[51,57]

Lastly, the effect of polymer chemistry on protein incorporation remains an open question. However, Blocher McTigue and Perry reported on the general effect of varying the charge density of the complexing polymers.[51] In this study, protein uptake was quantified using “fully charged” polypeptides of poly(lysine) and poly(glutamate). These results were then compared when one or both of the polypeptides was replaced with a “half-charged” polypeptide with an alternating sequence of the charged residue and neutral glycine. Consistent with electrostatic intuition, decreasing the charge density of the polypeptide with the same charge as the protein increased encapsulation efficiency by mitigating competition between the two species. Similarly, decreasing the charge density of the oppositely-charged polypeptide decreased uptake by intensifying this competition (Figures 10c,f). While these trends are interesting, more in-depth studies of the overall phase behavior of such systems is needed as a function of charge density, polymer chemistry, or perhaps even the specific sequence of charges on a polymer, to better understand the ways in which molecular-level details affect protein incorporation.

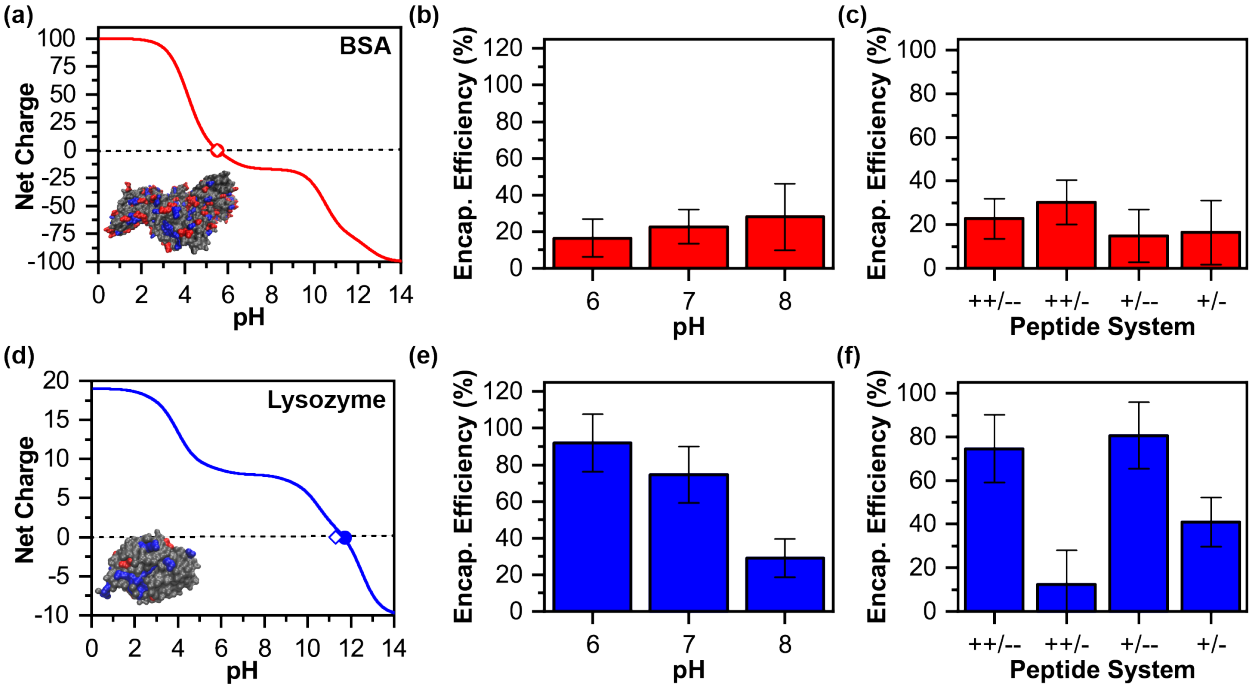

Figure 10. Theoretical charge calculations of **(a)** BSA and **(d)** lysozyme. Calculated values for the isoelectric point (pI) for each protein is indicated with filled circles, experimental data shown with open diamonds. The insets show 3D renderings of molecular models of BSA and lysozyme showing the distribution of positive (blue) and negative (red) charges on the protein surface. Encapsulation efficiency of **(b)** BSA and **(e)** lysozyme with increasing pH from 6 to 8. Encapsulation efficiency of **(c)** BSA and **(f)** lysozyme for different charged patterned peptides. (++) or (--) indicates a fully charged polycation or anion, respecitvely, with a total length of 50 charged amino acids while a single (+) or (-) indicates a half charged polycation or polyanion, respectively, as an alternating copolymer of charged or neutral amino acids. (Ref. 51, Blocher McTigue and Perry, Design Rules for Encapsulating Proteins into Complex Coacervates. *Soft Matter* **2019**, *15*, 3089–3103 – Reproduced by permission of The Royal Society of Chemistry.)

Although two-polymer systems have been shown to assist in protein encapsulation in bulk coacervates,[51] micellar morphologies that will not coalesce over time are desirable for delivery. Lindhoud and colleagues used oppositely charged block copolymers and homopolymers to encapsulate proteins in CCMs.[166-168] In the case of lysozyme, poly(acrylic acid)-*b*-poly(acrylamide) and poly(N,N-dimethylaminoethyl methacrylate) were used to form these micelles, sequestering lysozyme in the coacervate core.[167,168] Similar experiments were conducted with lipase using poly(acrylic acid) and poly(2-methylvinyl pyridinium)-*b*-poly(ethylene oxide).[166]

Protein Encapsulation and Release

Protein encapsulation is often a stepping-stone for another applications, and depending on the role of the protein, a specified release profile might be desired. Certain cases desire burst release, where all the protein cargo is released, while other applications require release over a specific, and possibly extended, amount of time. In the case of applications for drug delivery, controlled release is often desired. Complex coacervation has illustrated its ability to be tuned for these specific release parameters.[48,169,170] For example, Gao and co-workers encapsulated lysozyme and monitored its release at physiological ionic strength. They found a linear release of lysozyme over a 128 h period.[169] Additional work by Nishida *et al.* explored release of encapsulated proteins as a function of pH. For β-galactosidase, they observed higher activity at pH 5.0 than 7.4 and found a higher level of release at the more acidic pH over 24 h.[48] All of this work together suggests a complex interplay between the environment and the release of the

protein cargo. However, a more in depth discussion of drug delivery and release profiles are beyond the scope of this review.

Measuring Protein Concentration

While the discussion thus far has focused on the parameters associated with complex coacervation and phase behavior, the detection and quantification of the encapsulated proteins can also be a significant challenge. This challenge is particularly difficult because of the small volumes typical of many protein-containing coacervate samples. Unless high concentrations and volumes of polyelectrolyte are used, the coacervate phase is often very small (microliters) in volume. This can lead to difficulties in obtaining accurate concentrations and measureable volumes of the coacervate phase. Many systems utilize measurements of the protein concentration in the supernatant and an estimate of the coacervate volume to back calculate the amount of protein in the dense phase, as well as parameters such as the partitioning and encapsulation efficiency.

Traditional methods of determining protein concentration include indirect measurements using dye-based colorimetric readouts, such as the Bradford,[51,52] BCA,[171] and Lowry assays,[171] titration methods such as enzyme-linked immunosorbent assays (ELISA), and direct quantification via UV/Vis[56] or fluorescence spectrophotometry.[11,53,68,172] However, the choice of assay depends on the relevant concentration of protein in your sample, the ability to use or prepare a fluorescently-tagged protein, and the compatibility of the assay with the polymer materials present in the coacervate itself.

Colorimetric assays are a useful and relatively generic strategy for quantifying the concentration of proteins that do not have a unique spectroscopic signal, or are present at low concentrations in solution. Colorimetric assays detect proteins based on the presence of certain amino acids, but are typically unable to differentiate between multiple proteins. The reagents in the BCA (or bicinchoninic acid) assay react in the presence of cysteine, tyrosine, and tryptophan.[171] The Lowry assay works with the same amino acids as the BCA, as well as histidine and asparagine. The Coomassie brilliant blue G-250 dye associated with the Bradford assay is typically described as interacting with basic amino acids in hydrophobic pockets, but primarily responds to arginine residues, as well as histidine, tryptophan, tyrosine, and phenylalanine to a lesser extent.[171] The different assays each have varying strengths and weaknesses, particularly with regards to their compatibility with various reagents that might be present. However, to the best of our knowledge, only the Bradford and BCA assays have been used in the context of quantifying proteins in complex coacervates.[51,52,72,91] Although the coacervating polypeptides poly(lysine) and poly(glutamate) have been shown to work for the Bradford assay,[51,52] these same materials are not compatible with the BCA reagents, and more typical synthetic polymers such as poly(styrene sulfonate), poly(diallyldimethylammonium chloride), and other methacrylate based polymers have strong interactions with the assay reagents that overwhelm the ability of an experiment to detect protein. For a more detailed overview of these assays, we refer the reader to Ref. [162].

Outside of traditional colorimetric assays, the remaining reports that have quantified protein uptake into coacervates have largely used either UV/Vis spectroscopy to detect the protein directly via the signals from tyrosine and tryptophan residues at 280 nm,[56,57] or have taken advantage of a fluorescent signal (either natural as in the case of green fluorescent protein (GFP),[11] or synthetically conjugated).[52,91] UV/Vis measurements have the advantage of enabling quantification up to the very high concentrations (*e.g.*, 3,000 μg/mL),[173] but have relatively poor sensitivity at low concentrations. In contrast, fluorescence measurements are very sensitive at low concentrations, and are particularly useful for visualizing the presence of a protein. As with the use of colorimetric assays, the quantity of coacervate sample available for measurement can be limiting in many experiments. However, these limitations can be somewhat overcome through the use of microliter-scale drop-based methods that are becoming more common. Additionally, Brangwynne and co-workers have developed a method based on fluorescence correlation spectroscopy and confocal microscopy to infer information on protein concentration from microscopy samples.[13]

In the case of micellar systems, it can be difficult to detect the cargo, as it is hard to separate the micelles from free protein in solution. In these cases it might be useful to use similar bulk coacervates systems to determine concentration and then use a micellar system, though rigorous purification strategies might still be needed to validate micellar results. Lindhoud and co-workers have utilized small-

angle-neutron-scattering (SANS) to obtain information about the size, shape, and structure of micelle cores with and without protein.[166-168] However, it is difficult to obtain direct information concerning the number of protein molecules present without making assumptions about encapsulation efficiency.[166] Another potential method is to take advantage of fluorescence correlation spectroscopy, though the background fluorescence may hamper quantitative results.[64]

Encapsulation Efficiency, Partitioning, and Loading

Encapsulation efficiency (*EE*) is the percentage of cargo (by mass) sequestered, in this case, by complex coacervates:

$$EE = \frac{m_{coac.,cargo}}{m_{total\ cargo}} x100\% \quad (1)$$

A partition coefficient, on the other hand, is typically defined as the ratio of the concentration of the cargo in the dense coacervate phase over the concentration of the cargo in the dilute phase, written as:

$$K = \frac{[cargo_{coac.}]}{[cargo_{super.}]} \quad (2)$$

Finally, loading or loading capacity is the amount of cargo in the coacervate compared to everything else in the coacervate, *i.e.*, it describes what fraction of the coacervate phase is comprised of the cargo:

$$LC = \frac{m_{coac.,cargo}}{m_{coac.}} x100\% \quad (3)$$

All three parameters can be useful in describing the system. Encapsulation efficiency describes the amount of cargo that was sequestered into the dense phase, while loading capacity determines how much of the dense phase is made up of the cargo, and the partition coefficient describes the distribution of cargo between the two phases. In this sense, the encapsulation efficiency is effectively a function of the total amount of protein and polymer present in the system, and thus the relative volume of coacervate generated. In contrast, loading capacity and partitioning describe the thermodynamic distribution of protein in the various phases and are insensitive to coacervate volume. Thus, a combination of two of these parameters provides a fuller picture when determining the capacity of a system to incorporate protein cargo.

Experimentally, loading capacity and encapsulation efficiency can be very difficult to calculate when using low volumes as a direct measure of the coacervate mass is required and such small volumes are within noise for gravimetric balances. For this reason, these parameters are generally back-calculated based on the total protein content and the amount of protein remaining in the supernatant. In contrast, the concentration of protein in both the coacervate and supernatant can usually be measured, whether directly or via dissolution and dilution of the coacervate phase by the addition of salt, for instance. This means that the partition coefficient can be calculated directly.

Table 1 details papers that list encapsulation efficiency, along with corresponding protein cargo and polyelectrolytes chosen to make complex coacervates. Several additional papers discuss the encapsulation of proteins, but do not elaborate on the encapsulation efficiency.

Table 1. List of encapsulated proteins, the polyelectrolyte(s) used, the reported encapsulation efficiency (EE), and citation.

Protein	Polyanion/Polycation	EE (%)	Reference
β-galactosidase	poly(ethylene glycol)-block-poly(α ,β-aspartate acid), homo-([5-aminopentyl]- α , β-aspartamide)	0.9	[115]
	Methylated β-cyclodextrins-threaded acid-labile polyrotaxanes	15.5 – 24.4	[48]
Bovine serum albumin (BSA)	Chitosan	32.5 – 40.37	[72]
	poly(lysine), poly(glutamate)	100	[52]
	poly(allylamine hydrochloride), poly(acrylic aid)	15 – 50	[56]
	poly(L-lysine), poly(D/L-glutamate)	2.9 – 34.0	[51]
	Polyesters[a]	8.3 – 85.3	[71]
	Methylated β-cyclodextrins-threaded acid-labile polyrotaxanes	5.6 – 8.2	[48]
C. botulinum	Chitosan	41.03	[72]

type C toxoid			
C. botulinum type D toxoid	Chitosan	32.30	[72]
Curcumin	Bovine serum albumin, poly(D-lysine)	46.7 – 60.6	[66]
Ergosterol	Chitosan, whey protein	1.1 – 99.4	[174]
Fluorescent proteins	poly(2-methyl-vinyl-pyridinium)$_n$-block-poly(ethylene-oxide)$_m$	50 – 100	[67]
Green fluorescent protein	poly(styrenesulfonate), poly(acrylic acid), DNA, RNA	30 – >90	[11]
Human hemoglobin	poly(L-lysine), poly(D/L-glutamate)	0 – 25.5	[51]
Insulin	poly(ethylene glycol)-block-poly(L-lysine)	35 – 70	[110]
	Histidine-rich beak peptide	~100	[53]
Lysozyme	poly(2-methyl-vinyl-pyridinium)$_{128}$-block-poly(ethylene-oxide)$_{477}$	~100	[68]
	poly(L-lysine), poly(D/L-glutamate)	3.3 – 92.0	[51]
	Methylated β-cyclodextrins-threaded acid-labile polyrotaxanes	4.9 – 8.0	[48]
Zein	Chitosan	0.79 – 94.67	[175]

[a] Two of the thermoresponsive-polyesters were based on succinic acid/glutamic acid and N-substituted diols giving them a 12.5 or 15% positive charge on their repeat units.

Defining Protein Stability

In many cases, the encapsulation of proteins stems from a need to stabilize or protect the cargo. Applications that take advantage of proteins are particularly interested in the shelf life of the product, and how the protein responds to environmental changes such as temperature, humidity, light, etc. However, experiments often report information on two different types of stability: thermodynamic stability and kinetic stability.

Measuring Protein Stability

The use of the term “thermodynamic stability” can often lead to confusion as it is often conflated with “thermal stability,” which might or might not correspond to the shelf life of the protein at a given temperature. One reason for this confusion is that the thermodynamic stability is often characterized by the melting temperature (T_m) of a protein. However, other methods of determining stability include the addition of denaturing agents. The general premise of all of these methods is to identify a condition where half of the proteins are folded, and half of the proteins are unfolded, and thus the Gibbs free energy of unfolding $\Delta G_u = 0$.

In contrast with thermodynamic measures of the intrinsic stability of a molecule, kinetic stability refers to the “shelf life” of a protein, or the length of time over which a protein remains functional at a given set of conditions. Thus, for a majority of applications, shelf life might in fact be the preferred characteristic. However, determination of kinetic stability requires a time course of experiments that track changes in the folded structure and/or activity of the encapsulated protein. These experiments are more time and material intensive than thermodynamic measurements, as well as being less fundamental in nature, and are thus less common in the literature. Various correlations have been established to try and relate results from an accelerated aging experiment performed under harsher conditions. For instance, protein stability typically decreases with increasing temperature. Thus, one might be interested in the stability of a protein at 4°C, but instead of performing a three year experiment at refrigeration conditions, accelerated aging studies at a higher temperature could be used.[6] However, these types of correlations do not provide a guarantee of stability, and ultimately longer-term testing will be required.

Here, we will briefly introduce two methods, differential scanning calorimetry (DSC) and circular dichroism (CD) spectroscopy that have been used to characterize the thermodynamic stability of proteins encapsulated in complex coacervate-based materials. This discussion is not intended to be comprehensive, and other methods, such as differential scanning fluorimetry,[176-178] nuclear magnetic resonance (NMR) spectroscopy,[2,179] and hydrogen-deuterium exchange coupled with either NMR[23,179,180] or mass spectrometry (MS)[181,182] have also been used to characterize the stability of proteins generally. However, to the best of our knowledge these methods have not been used in the context of proteins encapsulated in coacervate materials to date. We will then compare the observed

trends in thermodynamic stability with those reported for kinetic stability based on direct measurements of protein activity over time.

Differential Scanning Calorimetry (DSC)

Differential scanning calorimetry (DSC) measures the difference in the absorption of heat between a sample cell and a reference cell as a function of temperature. Changes in the sample such as melting, boiling, or protein unfolding can then be detected because of the latent energy involved, and subsequent analysis allows for determination of thermodynamic data, such as the enthalpy and heat capacity of the protein.[183,184] In the context of protein unfolding, the melting temperature (T_m) is defined as the midpoint of the transition, where half of the protein is denatured and can be found as the peak in a thermogram of the heat flux or heat capacity versus temperature (Figure 11a).

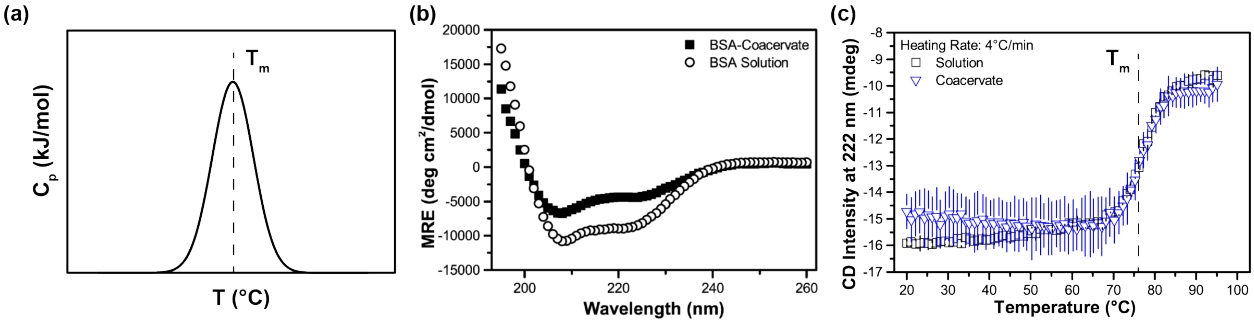

Figure 11. (a) Schematic depiction of a DSC thermogram. The dashed line represents the midpoint of the curve, which is used to determine the T_m. **(b)** CD spectra as a function of wavelength for BSA in solution and encapsulated in a complex coacervate of poly(lysine) and poly(glutamate) at a ratio of 0.05 BSA to total polypeptide. (Reprinted with permission from Ref. 52, Black, *et al.*, Protein encapsulation via polypeptide complex coacervation. *ACS Macro Lett.* **2014**, *3* (10). Copyright 2014 from the American Chemical Society.) **(c)** CD signal at 222 nm corresponding to the α-helical structure of lysozyme in solution and encapsulated in poly(lysine)/poly(glutamate) coacervates as a function of temperature. The dashed line represents the approximate midpoint of the curve, which corresponds to the T_m.

A variety of reports have utilized DSC to monitor how the thermodynamic stability of basic (*i.e.*, positively charged) proteins changed upon complexation with various polyanions.[185-187] Generally, the results showed that a decrease in the melting temperature was found upon complexation – meaning that the protein was less thermodynamically stable. This loss in thermodynamic stability may be caused by changes in the conformation of the cationic protein when complexed with a polyanion, as compared to its structure in solution. However, these measurements of thermodynamic stability were not correlated with shelf life measurements. Thus, it is not known whether or not complexation improves storage stability. Furthermore, it is not known whether complexation of these proteins with *all* polyanions might lead to a decrease in stability, or if a correctly tailored material environment with defined choice of polymer chemistry, sequence, and/or a mixture of polycations and polyanions might lead to a stabilizing result, as in the case of membraneless organelles in cells.

Circular Dichroism (CD) Spectroscopy

Another method to look at the secondary structure and stability of proteins is circular dichroism (CD) spectroscopy. This technique uses absorbance measurements from circularly polarized light to detect signals related to the secondary structure of proteins, typically in the range of 190 – 260 nm.[188,189] Details of secondary structure can be extracted through the use of basis spectra that describe typical protein conformations, such as α-helix, β-sheet, and random coil. Each of these prototypical secondary structure elements can be described by characteristic minima and/or maxima, and fitting procedures can be used to calculate the amount of each structure in a given protein, and potentially the change in that structure. Figure 11b shows the CD spectra for the primarily α-helical protein BSA, showing the characteristic

double minima at 208 nm and 222 nm, as well as the large increase in absorbance at low wavelength.[52] Additionally, because CD relies on the absorbance of light, it can also be used to simultaneously measure protein concentration and stability.[190] For more information on CD, we refer the reader to Ref. [181].

For determination of thermodynamic stability, the absorbance at a single characteristic wavelength is typically monitored as a function of temperature or denaturant, although full characterization of the spectra can also be performed. Similar to DSC, the melting temperature would then be defined as the midpoint in the unfolding curve (Figure 11c). It should be noted that for DSC, CD, or any other method, the melting temperature is only a *true* measure of thermodynamic stability if the protein can be first reversibly unfolded, and then refolded, as the analysis described here assumes a single step reaction coordinate where the protein converts from its native state to an unfolded state. Nevertheless, the single (irreversible) heating curves typical of most studies will still provide information about protein stability.

Several groups have utilized CD as a means of detecting conformational changes of proteins with complex coacervates.[52,91,142,149,151,191] Full spectral analysis has often been used to validate that complex coacervation did not change the secondary structure of the encapsulated cargo (Figure 11b).[52,172] Mazzaferro and colleagues used CD to determine whether the melting point (T_m) changed for a series of acidic and basic proteins of lactate dehydrogenase, human serum albumin (HSA), cutinase, human recombinant growth hormone, lysozyme, and ribonuclease A when complexed with polyethyleneimine (PEI) or sorbitol.[192] Interestingly, the authors found that in some instances the T_m decreased, while in others it was increased, indicating that the specific protein and polyelectrolyte play crucial roles in determining stability. For instance, when HSA was complexed with PEI, the T_m decreased from 81°C to 72°C; however, the T_m increased (>95°C) when HSA complexed with sorbitol.[192] When HSA was complexed with both PEI and sorbitol at the same time, the T_m only had a slight increase to 86°C, which is between the T_m reported for each system individually.

Lastly, it should be noted that both DSC and CD require that the measurement not be affected by the presence of the coacervate materials. Thus, absorbance signals from protein or polypeptide-based polymers could interfere with CD measurements, as could melting or restructuring phenomena associated with the polymers. However, these considerations can easily be tested with a control sample lacking protein. Unique to the case of polypeptide-based coacervates, the use of racemic (*i.e.*, a mixture of *D* and *L* enantiomers) peptides results in equal right- and left-handed contributions to the CD spectrum, thus eliminating signal from the background matrix.[74]

Determining Kinetic Stability

Rather than focusing on the structure of a protein, studies of the kinetic stability of a protein require a readout that demonstrates the activity or efficacy of the protein. Several groups have utilized enzymatic and other assays to determine the stability of proteins at certain temperatures with respect to time. For example, Shaddel and co-workers used complex coacervation to improve stability of anthocyanins at 37°C for two months with gelatin and gum Arabic.[193] A large number of studies have also been performed for proteins incorporated into polyion complex vesicles, or PICsomes. Tang and co-workers incubated the complexes at 37°C, 4°C, and -20°C for 24 h and found that enzyme stability was increased at 37°C with high enzyme concentration compared to being in solution.[61] Additionally, the co-encapsulation of dextran allowed for an improved shelf life at -20°C as shown with increased stability after 7 days. Sueyoshi and colleagues also utilized PICsomes and found enzyme to remain active after 24 h at 37°C.[194] Longer studies conducted by Filatova and co-workers illustrated the ability for phage K endolysin to be stable at 37°C, 22°C, and 4°C for several hours, days, and months, respectively, improving upon the native stability.[195]

It is interesting to see that in the case of thermal stability, as defined above, there have been reports describing decrease in stability with T_m, but an increase in stability in terms of storage. Filatova and co-workers see this with an endolysin of the staphylococcal bacteriophage phage K.[195] This is an interesting dynamic between thermodynamic and storage stabilities that could play large roles in formulation for and use of protein encapsulation in various applications. The use of either metric of temperature stability can give insight to the nature of the protein. Comparison of these measurements can detect if coacervate formulations negatively affect the cargo and if such systems are useful for long-term storage at specific temperatures. For both types of stability, the environment can have profound effects.

Learning from Nature

Tuning the Environment for Protein Uptake

The changing of the local milieu heavily affects the electrostatic driving force for complex coacervation, but may not necessarily lead to the uptake of a specific protein. Incorporation will likely be heavily determined by the charge nature of the polyelectrolytes used, the charge level and distribution of charge on the protein, as well as the relative concentrations of all the various species present. Just as membraneless organelles have evolved to facilitate uptake of specific proteins and/or RNAs,[19,20,156,196-200] variety of reports have described the use of complex coacervation to separate or purify proteins.[10,51,137,142,201,202]

Probably the most dramatic example of selective protein uptake is the coacervation-based separation of two isoforms of β-lactoglobulin (BLG-A and BLG-B).[142,201] These two isoforms vary only with the amino acid content at positions 64 and 118. In BLG-A these residues are aspartate (D) and valine (V), respectively, and glycine (G) and alanine (A), respectively, for BLG-B. These amino acids translate to a difference of only a single negative charge (from the aspartate), corresponding to a change in the pI by 0.1 pH units (Figure 12a,b). The authors took advantage of this very slight difference in the charge state, forming a coacervate with the addition of a polycation such as poly(diallyldimethylammonium chloride) (PDADMAC)[142] or lactoferrin[201] that was enriched in the slightly more negative isoform, BLG-A (Figure 12c).

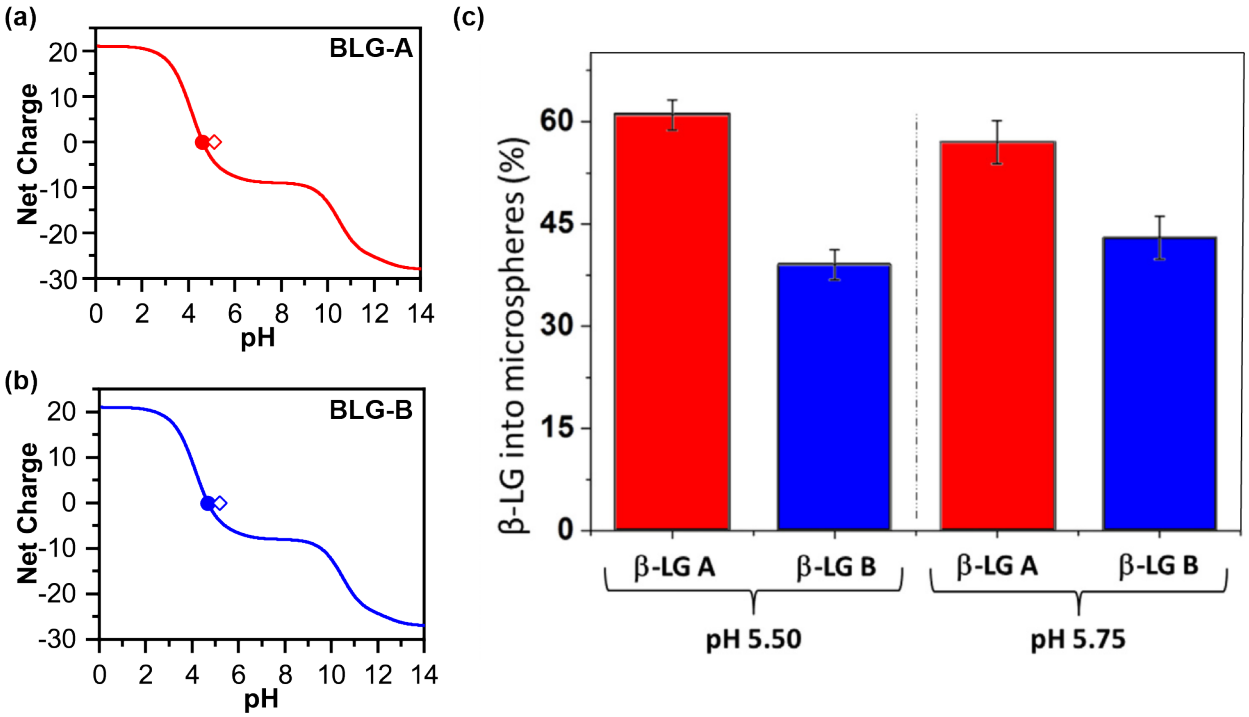

Figure 12. Theoretical charge calculations for two isoforms of β-lactoglobulin, **(a)** BLG-A and **(b)** BLG-B. The calculated value of the pI for BLG-A and BLG-B was 4.6 and 4.7, respectively (filled circles). Experimental values of the pI from the literature reported 5.1 and 5.2, respectively (open diamonds). **(c)** Proportion of BLG-A (red) and BLG-B (blue) into the coacervte phase mixing lacftoferrin and BLG-A + B at pH 5.50 and 5.75. (Reprinted from Ref. 201, Tavares, *et al.*, Selective coacervation between lactoferrin and the two isoforms of beta-lactoglobulin. *Food Hydrocolloids* **2015**, *48*, 238–247,with permission from Elsevier.)

Dubin and co-workers also demonstrated that protein affinity for complex coacervation could be changed with respect to pH and ionic strength between two different proteins, β-lactoglobulin (BLG) and

bovine serum albumin (BSA) in complex with poly(diallyldimethylammonium chloride) (PDADMAC).[142] BLG preferentially coacervates at ionic strength above 50 mM, whereas the affinity of PDADMAC for BSA decreases above 50 mM. At high salt (>5 mM) BSA does not coacervate with PDADMAC until a pH above 7, unlike BLG, which can coacervate with PDADMAC just above pH 6 with a wide range of salt. The differences in the behavior of these two proteins was attributed to differences in the distribution of charge. BSA has charges distributed across its surface with a reported pI of 4.9, whereas BLG has a distinct charge patch (Figure 13). The authors demonstrated that the charge patch present on BLG allowed most of the protein to preferentially go into the coacervate phase via electrostatic attraction, while the majority of BSA remained in the supernatant (*i.e.*, at 100 mM ionic strength and pH 7, 90% of the BLG was incorporated into the dense phase with 85% of the BSA remaining in the supernatant phase). Salt and pH were chosen based on the region of these data highlight the important role that chemical sequence and charge patches play in defining protein interactions. However, more comprehensive, broader efforts are needed to understand the subtle, molecular-level strategies that nature has developed to control protein localization.

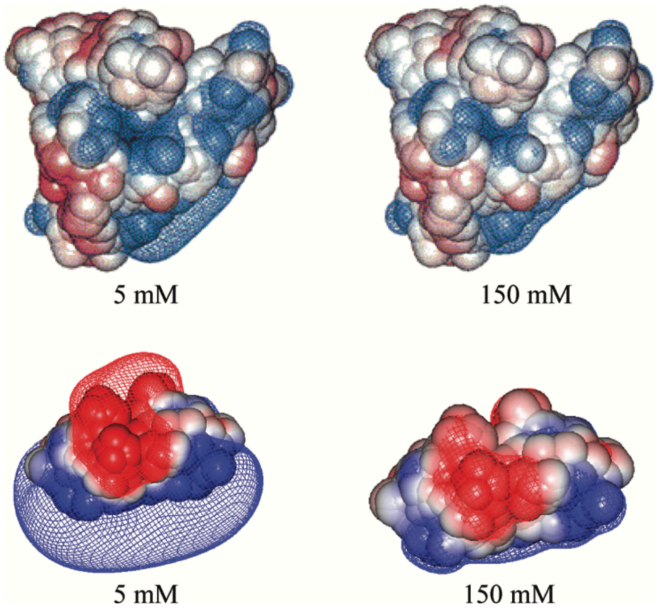

Figure 13. Electrostatic potential contours (-0.5 (red) and +0.5 (blue) kT/e) for BSA (upper) at pH 5.6 and BLG dimer (lower) at pH 5.0. The charges are distributed around BSA, while BLG has a distinct negatively charged patch on the top and positive patch on the bottom. (Reprinted with permission from Ref. 142, Xu, *et al.*, Protein Purification by Polyelectrolyte Coacervation: Influence of Protein Charge Anisotropy on Selectivity. *Biomacromolecules* **2011**, *12* (5), 1512–1522. Copyright 2011 from the American Chemical Society.)

Summary and Outlook

There is a growing recognition of the potential for using complex coacervates as an all-aqueous, bioinspired strategy for protein encapsulation. The phase behavior of complex coacervates is broadly tunable through changes in polymer chemistry, length, charge density, and charge sequence, as well as solution conditions. This flexibility, along with parallel examples of liquid-liquid phase separated organelles in cells has the potential to allow for the incorporation of many of the (presumably stabilizing) qualities of the native protein environment. Furthermore, these materials have been shown to concentrate proteins, potentially for use in the formulation of therapeutics, as well as for wide-ranging applications in purification and beyond.

Here, we have attempted to summarize current knowledge in the field with regards to complex coacervation alone, as well as the added complications associated with proteins as more complex charged species. However, from this discussion we would also argue that more fundamental studies are needed to understand how the subtle molecular-level details that natural systems have evolved to use can be harnessed in synthetic systems to enhance protein incorporation and potentially stability or activity. In particular, we would like to highlight potential areas where this type of nature-inspired complexity could have a dramatic effect. Firstly, reports on the formation of membraneless organelles and have begun to explore the ways in which chemical sequence on both the protein and on the coacervating IDPs (polymers) can be used to selectively uptake specific targets out of the complex mixture of the cytosol. Such knowledge could be harnessed to improve protein purification efforts, as well as enhancing protein loading for drug delivery applications. Secondly, very little is known about the ways in which complex, multi-species mixtures interact. The potential to identify strategies to selectively and simultaneously sequester different proteins and/or their substrates/products could have significant ramifications for the development of protein-based nanobioreactors. Lastly, the formulation questions that we have raised here can be brought to the drug delivery field, allowing for the selective delivery and release of cargo through a variety of mechanisms.

Because the breadth of this potential experimental space is vast, these types of questions may best be answered by collaborative efforts that use experimental data to validate predictive models based on fundamental physics and/or machine learning strategies to sift through large quantities of data to extract trends.

Acknowledgements

W.C.B.M. was supported by a Fellowship from the Soft Materials for Life Sciences National Research Traineeship Program #NRT-1545399. We would also like to thank PPG for funding support of W.C.B.M. through a grant to the Department of Chemical Engineering at the University of Massachusetts Amherst.

References

[1] M. Sarkar, C. Li, G. J. Pielak, *Biophys Rev* **2013**, *5*, 187.
[2] Y. Wang, M. Sarkar, A. E. Smith, A. S. Krois, G. J. Pielak, *J Am Chem Soc* **2012**, *134*, 16614.
[3] S. B. Zimmerman, S. O. Trach, *J. Mol. Biol.* **1991**, *222*, 599.
[4] A. B. Fulton, *Cell* **1982**, *30*, 345.
[5] S. R. McGuffee, A. H. Elcock, *PLoS Comput Biol* **2010**, *6*, e1000694.
[6] A. Galazka, J. Milstien, M. Zaffran, *Thermostability of Vaccines*, World Health Organization, Geneva, Switzerland, **1998**.
[7] World Health Organization, *WHO Model List of Essential Medicines: 19th List, April 2015*, **2013**.
[8] S. L. Perry, *Curr. Opin. Colloid Interface Sci.* **2019**, *39*, 86.
[9] B. Panganiban, B. Qiao, T. Jiang, C. DelRe, M. M. Obadia, T. D. Nguyen, A. A. A. Smith, A. Hall, I. Sit, M. G. Crosby, P. B. Dennis, E. Drockenmuller, M. Olvera de la Cruz, T. Xu, *Science* **2018**, *359*, 1239.
[10] J. J. van Lente, M. M. A. E. Claessens, S. Lindhoud, *Biomacromolecules* **2019**, *20*, 3696.
[11] C. S. Cummings, A. C. Obermeyer, *Biochemistry* **2018**, *57*, 314.
[12] R. A. Kapelner, A. C. Obermeyer, *Chem. Sci.* **2019**, *10*, 2700.
[13] M.-T. Wei, S. Elbaum-Garfinkle, A. S. Holehouse, C. C.-H. Chen, M. Feric, C. B. Arnold, R. D. Priestley, R. V. Pappu, C. P. Brangwynne, *Nat Chem* **2017**, *9*, 1118.
[14] C. F. Lee, C. P. Brangwynne, J. Gharakhani, A. A. Hyman, F. Jülicher, *Phys. Rev. Lett.* **2013**, *111*, 1287.
[15] T. J. Nott, T. D. Craggs, A. J. Baldwin, *Nat Chem* **2016**, *8*, 569.
[16] T. J. Nott, E. Petsalaki, P. Farber, D. Jervis, E. Fussner, A. Plochowietz, T. D. Craggs, D. P. Bazett-Jones, T. Pawson, J. D. Forman-Kay, A. J. Baldwin, *Mol. Cell* **2015**, *57*, 936.
[17] C. W. Pak, M. Kosno, A. S. Holehouse, S. B. Padrick, A. Mittal, R. Ali, A. A. Yunus, D. R. Liu, R. V. Pappu, M. K. Rosen, *Mol. Cell* **2016**, *63*, 72.
[18] S. F. Banani, H. O. Lee, A. A. Hyman, M. K. Rosen, *Nat. Rev. Mol. Cell Biol.* **2017**, *18*, 285.
[19] F. Wippich, B. Bodenmiller, M. G. Trajkovska, S. Wanka, R. Aebersold, L. Pelkmans, *Cell*

2013, *152*, 791.
[20] A. Molliex, J. Temirov, J. Lee, M. Coughlin, A. P. Kanagaraj, H. J. Kim, T. Mittag, J. P. Taylor, *Cell* **2015**, *163*, 123.
[21] S. An, R. Kumar, E. D. Sheets, S. J. Benkovic, *Science* **2008**, *320*, 103.
[22] A. M. Pedley, S. J. Benkovic, *Trends Biochem Sci* **2017**, *42*, 141.
[23] R. D. Cohen, G. J. Pielak, *Prot Sci* **2017**, *26*, 403.
[24] D. J. McClements, *Adv. Colloid Interface Sci.* **2018**, *253*, 1.
[25] C. Ye, H. Chi, *Mater. Sci. Eng., C* **2018**, *83*, 233.
[26] C. D. Spicer, C. Jumeaux, B. Gupta, M. M. Stevens, *Chem. Soc. Rev.* **2018**, 3574.
[27] M. B. Dowling, A. S. Bagal, S. R. Raghavan, *Langmuir* **2013**, *29*, 7993.
[28] M. R. Molla, T. Marcinko, P. Prasad, D. Deming, S. C. Garman, S. Thayumanavan, *Biomacromolecules* **2014**, *15*, 4046.
[29] P. N. Kendre, T. S. Satav, *Polym Bull* **2018**, *76*, 1595.
[30] J.-H. Ryu, R. T. Chacko, S. Jiwpanich, S. Bickerton, R. P. Babu, S. Thayumanavan, *J Am Chem Soc* **2010**, *132*, 17227.
[31] V. R. Sinha, A. Trehan, *J. Controlled Release* **2003**, *90*, 261.
[32] H. Kawaguchi, *Prog Polym Sci* **2000**, *25*, 1171.
[33] D. S. Pisal, M. P. Kosloski, S. V. Balu-Iyer, *J. Pharm. Sci.* **2010**, *99*, 2557.
[34] S. Martins, B. Sarmento, D. C. Ferreira, E. B. Souto, *Int. J. Nanomed.* **2007**, *2*, 595.
[35] M. L. Tan, P. F. M. Choong, C. R. Dass, *Peptides* **2010**, *31*, 184.
[36] A. Yamada, T. Yamanaka, T. Hamada, M. Hase, K. Yoshikawa, D. Baigl, *Langmuir* **2006**, *22*, 9824.
[37] R. K. Shah, H. C. Shum, A. C. Rowat, D. Lee, J. J. Agresti, A. S. Utada, L.-Y. Chu, J. W. Kim, A. Fernandez-Nieves, C. J. Martinez, D. A. Weitz, *Materials Today* **2008**, *11*, 18.
[38] M. Michelon, Y. Huang, L. G. de la Torre, D. A. Weitz, R. L. Cunha, *Chemical Engineering Journal* **2019**, *366*, 27.
[39] C. D. Keating, *Acc. Chem. Res.* **2012**, *45*, 2114.
[40] B. W. Davis, W. M. Aumiller Jr, N. Hashemian, S. An, A. Armaou, C. D. Keating, *Biophys. J.* **2015**, *109*, 2182.
[41] L. M. Dominak, E. L. Gundermann, C. D. Keating, *Langmuir* **2010**, *26*, 5697.
[42] E. W. Martin, T. Mittag, *Biochemistry* **2018**, *57*, 2478.
[43] A. Chilkoti, T. Christensen, J. A. MacKay, *Curr. Opin. Chem. Biol.* **2006**, *10*, 652.
[44] S. Roberts, M. Dzuricky, A. Chilkoti, *FEBS Lett.* **2015**, *589*, 2477.
[45] N. R. Johnson, Y. Wang, *Expert Opin. Drug Delivery* **2014**, *11*, 1829.
[46] N. R. Johnson, Y. Wang, *J. Controlled Release* **2013**, *166*, 124.
[47] H. Cabral, K. Miyata, K. Osada, K. Kataoka, *Chemical Reviews* **2018**, *118*, 6844.
[48] K. Nishida, A. Tamura, N. Yui, *Biomacromolecules* **2018**, *19*, 2238.
[49] A.-L. Chapeau, N. Bertrand, V. Briard-Bion, P. Hamon, D. Poncelet, S. Bouhallab, *J Funct Foods* **2017**, *38*, 197.
[50] V. Bourganis, T. Karamanidou, O. Kammona, C. Kiparissides, *Eur J Pharm Biopharm* **2017**, *111*, 44.
[51] W. C. Blocher McTigue, S. L. Perry, *Soft Matter* **2019**, *15*, 3089.
[52] K. A. Black, D. Priftis, S. L. Perry, J. Yip, W. Y. Byun, M. Tirrell, *ACS Macro Lett.* **2014**, *3*, 1088.
[53] Z. W. Lim, Y. Ping, A. Miserez, *Bioconjugate Chem.* **2018**, *29*, 2176.
[54] M. B. Santos, C. W. P. de Carvalho, E. E. Garcia- Rojas, *Food Hydrocolloids* **2018**, *74*, 267.
[55] T. Croguennec, G. M. Tavares, S. Bouhallab, *Adv. Colloid Interface Sci.* **2017**, *239*, 115.
[56] M. Zhao, N. S. Zacharia, *J Chem Phys* **2018**, *149*, 163326.
[57] S. Lindhoud, M. M. A. E. Claessens, *Soft Matter* **2016**, *12*, 408.
[58] G. L. Bidwell III, D. Raucher, *Adv. Drug Delivery Rev.* **2010**, *62*, 1486.
[59] I. Massodi, G. L. Bidwell III, D. Raucher, *J. Controlled Release* **2005**, *108*, 396.
[60] S. Pacelli, P. Paolicelli, M. A. Casadei, *Carbohydr. Polym.* **2015**, *126*, 208.
[61] H. Tang, Y. Sakamura, T. Mori, Y. Katayama, A. Kishimura, *Macromol. Biosci.* **2017**, *5*, 1600542.
[62] D. Garenne, L. Beven, L. Navailles, F. Nallet, E. J. Dufourc, J.-P. Douliez, *Angew. Chem.* **2016**, *128*, 13673.

[63] Y. Zhang, K. Han, D. Lu, Z. Liu, *Soft Matter* **2013**, *9*, 8723.
[64] A. Nolles, A. H. Westphal, J. A. de Hoop, R. G. Fokkink, J. M. Kleijn, W. J. H. van Berkel, J. W. Borst, A. H. Westphal, *Biomacromolecules* **2015**, *16*, 1542.
[65] K. Kataoka, A. Harada, Y. Nagasaki, *Adv. Drug Delivery Rev.* **2001**, *47*, 113.
[66] L. Maldonado, R. Sadeghi, J. Kokini, *Colloids Surf, B* **2017**, *159*, 759.
[67] A. Nolles, A. Westphal, J. Kleijn, W. van Berkel, J. Borst, *Int. J. Mol. Sci.* **2017**, *18*, 1557.
[68] A. Nolles, E. Hooiveld, A. H. Westphal, W. J. H. van Berkel, J. M. Kleijn, J. W. Borst, *Langmuir* **2018**, *34*, 12083.
[69] A. K. Andrianov, A. Marin, A. P. Martinez, J. L. Weidman, T. R. Fuerst, *Biomacromolecules* **2018**, *19*, 3467.
[70] D. Eratte, K. Dowling, C. J. Barrow, B. Adhikari, *Trends Food Sci Technol* **2018**, *71*, 121.
[71] M. A. Cruz, D. L. Morris, J. P. Swanson, M. Kundu, S. G. Mankoci, T. C. Leeper, A. Joy, *ACS Macro Lett.* **2018**, *7*, 477.
[72] R. S. Sari, A. C. de Almeida, A. S. R. Cangussu, E. V. Jorge, O. D. Mozzer, H. O. Santos, W. Quintilio, I. V. Brandi, V. A. Andrade, A. S. M. Miguel, E. M. S. Santos, *Anaerobe* **2016**, *42*, 182.
[73] C. E. Sing, S. L. Perry, *Soft Matter* **2020**, *50*, 9528.
[74] S. L. Perry, L. Leon, K. Q. Hoffmann, M. J. Kade, D. Priftis, K. A. Black, D. Wong, R. A. Klein, C. F. Pierce, K. O. Margossian, J. K. Whitmer, J. Qin, J. J. de Pablo, M. Tirrell, *Nat Commun* **2015**, *6*, 6052.
[75] D. Priftis, L. Leon, Z. Song, S. L. Perry, K. O. Margossian, A. Tropnikova, J. Cheng, M. Tirrell, *Angew. Chem.* **2015**, *127*, 11280.
[76] S. Perry, Y. Li, D. Priftis, L. Leon, M. Tirrell, *Polymers* **2014**, *6*, 1756.
[77] D. Priftis, X. Xia, K. O. Margossian, S. L. Perry, L. Leon, J. Qin, J. J. de Pablo, M. Tirrell, *Macromolecules* **2014**, *47*, 3076.
[78] S. L. Perry, S. G. Neumann, T. Neumann, K. Cheng, J. Ni, J. R. Weinstein, D. V. Schaffer, M. Tirrell, *AIChE J.* **2013**, *59*, 3203.
[79] D. Priftis, K. Megley, N. Laugel, M. Tirrell, *J. Colloid Interface Sci.* **2013**, *398*, 39.
[80] R. Chollakup, W. Smitthipong, C. D. Eisenbach, M. Tirrell, *Macromolecules* **2010**, *43*, 2518.
[81] R. Chollakup, J. B. Beck, K. Dirnberger, M. Tirrell, C. D. Eisenbach, *Macromolecules* **2013**, *46*, 2376.
[82] D. Priftis, R. Farina, M. Tirrell, *Langmuir* **2012**, *28*, 8721.
[83] D. Priftis, M. Tirrell, *Soft Matter* **2012**, *8*, 9396.
[84] D. Priftis, N. Laugel, M. Tirrell, *Langmuir* **2012**, *28*, 15947.
[85] E. Spruijt, M. A. Cohen Stuart, J. van der Gucht, *Macromolecules* **2013**, *46*, 1633.
[86] E. Spruijt, A. H. Westphal, J. W. Borst, M. A. Cohen Stuart, J. van der Gucht, *Macromolecules* **2010**, *43*, 6476.
[87] L. Li, S. Srivastava, M. Andreev, A. B. Marciel, J. J. de Pablo, M. V. Tirrell, *Macromolecules* **2018**, *51*, 2988.
[88] A. B. Kayitmazer, A. F. Koksal, E. K. Iyilik, *Soft Matter* **2015**, *11*, 8605.
[89] M. Radhakrishna, K. Basu, Y. Liu, R. Shamsi, S. L. Perry, C. E. Sing, *Macromolecules* **2017**, *50*, 3030.
[90] Y. Liu, H. H. Winter, S. L. Perry, *Adv. Colloid Interface Sci.* **2017**, *239*, 46.
[91] A. C. Obermeyer, C. E. Mills, X.-H. Dong, R. J. Flores, B. D. Olsen, *Soft Matter* **2016**, *12*, 3570.
[92] J. van der Gucht, E. Spruijt, M. Lemmers, M. A. Cohen Stuart, *J. Colloid Interface Sci.* **2011**, *361*, 407.
[93] S. Ali, M. Bleuel, V. M. Prabhu, *ACS Macro Lett.* **2019**, *8*, 289.
[94] W. M. Aumiller Jr, C. D. Keating, *Nat Chem* **2015**, *8*, 129.
[95] J. J. Madinya, L.-W. Chang, S. L. Perry, C. E. Sing, *Mol. Syst. Des. Eng.* **2019**, Accepted.
[96] S. L. Perry, C. E. Sing, *Macromolecules* **2015**, *48*, 5040.
[97] J. Qin, D. Priftis, R. Farina, S. L. Perry, L. Leon, J. Whitmer, K. Hoffmann, M. Tirrell, J. J. de Pablo, *ACS Macro Lett.* **2014**, *3*, 565.
[98] L.-W. Chang, T. K. Lytle, M. Radhakrishna, J. J. Madinya, J. Vélez, C. E. Sing, S. L. Perry, *Nat Commun* **2017**, *8*, 1273.
[99] T. K. Lytle, L.-W. Chang, N. Markiewicz, S. L. Perry, C. E. Sing, *ACS Cent Sci* **2019**, *5*, 709.

[100] S. P. O. Danielsen, J. McCarty, J.-E. Shea, K. T. Delaney, G. H. Fredrickson, *PNAS* **2019**, *116*, 8224.
[101] S. Tabandeh, L. Leon, *Molecules* **2019**, *24*, 868.
[102] K. Sadman, Q. Wang, Y. Chen, B. Keshavarz, Z. Jiang, K. R. Shull, *Macromolecules* **2017**, *50*, 9417.
[103] J. Lou, S. Friedowitz, J. Qin, Y. Xia, *ACS Cent Sci* **2019**, *5*, 549.
[104] K. Q. Hoffmann, S. L. Perry, L. Leon, D. Priftis, M. Tirrell, J. J. de Pablo, *Soft Matter* **2015**, *11*, 1525.
[105] N. M. Pacalin, L. Leon, M. Tirrell, *Eur. Phys. J. Spec. Top.* **2016**, *225*, 1805.
[106] J. Wang, J.-M. Choi, A. S. Holehouse, H. O. Lee, X. Zhang, M. Jahnel, S. Maharana, R. Lemaitre, A. Pozniakovsky, D. Drechsel, I. Poser, R. V. Pappu, S. Alberti, A. A. Hyman, *Cell* **2018**, *174*, 688.
[107] F. Comert, A. J. Malanowski, F. Azarikia, P. L. Dubin, *Soft Matter* **2016**, *12*, 4154.
[108] R. K. Das, R. V. Pappu, *PNAS* **2013**, *110*, 13392.
[109] Y.-H. Lin, J. D. Forman-Kay, H. S. Chan, *Phys. Rev. Lett.* **2016**, *117*, 1201.
[110] N. Pippa, R. Kalinova, I. Dimitrov, S. Pispas, C. Demetzos, *J. Phys. Chem. B* **2015**, *119*, 6813.
[111] N. Bourouina, M. A. Cohen Stuart, J. M. Kleijn, *Soft Matter* **2014**, *10*, 320.
[112] N. Bourouina, D. W. de Kort, F. J. M. Hoeben, H. M. Janssen, H. Van As, J. Hohlbein, J. P. M. van Duynhoven, J. M. Kleijn, *Langmuir* **2015**, *31*, 12635.
[113] Y. Anraku, A. Kishimura, Y. Yamasaki, K. Kataoka, *J Am Chem Soc* **2013**, *135*, 1423.
[114] Y. Anraku, A. Kishimura, M. Oba, Y. Yamasaki, K. Kataoka, *J Am Chem Soc* **2010**, *132*, 1631.
[115] Y. Anraku, A. Kishimura, M. Kamiya, S. Tanaka, T. Nomoto, K. Toh, Y. Matsumoto, S. Fukushima, D. Sueyoshi, M. R. Kano, Y. Urano, N. Nishiyama, K. Kataoka, *Angew. Chem.* **2015**, *128*, 570.
[116] U. Kwolek, K. Nakai, A. Pluta, M. Zatorska, D. Wnuk, S. Lasota, J. Bednar, M. Michalik, S.-I. Yusa, M. Kepczynski, *Colloids Surf, B* **2017**, *158*, 658.
[117] W. C. Blocher, S. L. Perry, *WIREs Nanomed Nanobiotechnol* **2017**, *9*, e1442.
[118] J. N. Hunt, K. E. Feldman, N. A. Lynd, J. Deek, L. M. Campos, J. M. Spruell, B. M. Hernandez, E. J. Kramer, C. J. Hawker, *Adv. Mater.* **2011**, *23*, 2327.
[119] D. V. Krogstad, N. A. Lynd, S.-H. Choi, J. M. Spruell, C. J. Hawker, E. J. Kramer, M. V. Tirrell, *Macromolecules* **2013**, *46*, 1512.
[120] D. V. Krogstad, S.-H. Choi, N. A. Lynd, D. J. Audus, S. L. Perry, J. D. Gopez, C. J. Hawker, E. J. Kramer, M. V. Tirrell, *J. Phys. Chem. B* **2014**, *118*, 13011.
[121] J. H. Ortony, S.-H. Choi, J. M. Spruell, J. N. Hunt, N. A. Lynd, D. V. Krogstad, V. S. Urban, C. J. Hawker, E. J. Kramer, S. Han, *Chem. Sci.* **2014**, *5*, 58.
[122] D. V. Krogstad, N. A. Lynd, D. Miyajima, J. Gopez, C. J. Hawker, E. J. Kramer, M. V. Tirrell, *Macromolecules* **2014**, *47*, 8026.
[123] B. K. Ahn, S. Das, R. Linstadt, Y. Kaufman, N. R. Martinez-Rodriguez, R. Mirshafian, E. Kesselman, Y. Talmon, B. H. Lipshutz, J. N. Israelachvili, J. H. Waite, *Nat Commun* **2015**, *6*, 8663.
[124] Q. Wang, J. B. Schlenoff, *Macromolecules* **2014**, *47*, 3108.
[125] H. Kinoh, Y. Miura, T. Chida, X. Liu, K. Mizuno, S. Fukushima, Y. Morodomi, N. Nishiyama, H. Cabral, K. Kataoka, *ACS Nano* **2016**, *10*, 5643.
[126] H. Cabral, J. Makino, Y. Matsumoto, P. Mi, H. Wu, T. Nomoto, K. Toh, N. Yamada, Y. Higuchi, S. Konishi, M. R. Kano, H. Nishihara, Y. Miura, N. Nishiyama, K. Kataoka, *ACS Nano* **2015**, *9*, 4957.
[127] E. Ghorbani Gorji, A. Waheed, R. Ludwig, J. L. Toca-Herrera, G. Schleining, S. Ghorbani Gorji, *J. Agric. Food Chem.* **2018**, *66*, 3210.
[128] A.-L. Chapeau, G. M. Tavares, P. Hamon, T. Croguennec, D. Poncelet, S. Bouhallab, *Food Hydrocolloids* **2016**, *57*, 280.
[129] A.-L. Chapeau, P. Hamon, F. Rousseau, T. Croguennec, D. Poncelet, S. Bouhallab, *J. Food Eng.* **2017**, *206*, 67.
[130] C. Sanchez, G. Mekhloufi, C. Schmitt, D. Renard, P. Robert, C. M. Lehr, A. Lamprecht, J. Hardy, *Langmuir* **2002**, *18*, 10323.
[131] S. L. Turgeon, M. Beaulieu, C. Schmitt, C. Sanchez, *Curr. Opin. Colloid Interface Sci.* **2003**, *8*, 401.

[132] C. Schmitt, S. L. Turgeon, *Adv. Colloid Interface Sci.* **2011**, *167*, 63.
[133] S. L. Turgeon, C. Schmitt, C. Sanchez, *Curr. Opin. Colloid Interface Sci.* **2007**, DOI 10.1016/j.cocis.2007.07.007.
[134] E. Gasteiger, C. Hoogland, A. Gattiker, S. Duvaud, M. R. Wilkins, R. D. Appel, A. Bairoch, *The Proteomics Protocols Handbook*, Humana Press, **2005**.
[135] C. L. Cooper, P. L. Dubin, A. B. Kayitmazer, S. Turksen, *Curr. Opin. Colloid Interface Sci.* **2005**, *10*, 52.
[136] X. Du, P. L. Dubin, D. A. Hoagland, L. Sun, *Biomacromolecules* **2014**, *15*, 726.
[137] P. L. Dubin, J. Gao, K. Mattison, *Separation & Purification Reviews* **1994**, *23*, 1.
[138] A. B. Kayitmazer, D. Seeman, B. B. Minsky, P. L. Dubin, Y. Xu, *Soft Matter* **2013**, *9*, 2553.
[139] E. Kizilay, A. B. Kayitmazer, P. L. Dubin, *Adv. Colloid Interface Sci.* **2011**, *167*, 24.
[140] C. G. de Kruif, F. Weinbreck, R. de Vries, *Curr. Opin. Colloid Interface Sci.* **2004**, *9*, 340.
[141] J. Pathak, K. Rawat, H. B. Bohidar, *RSC Adv.* **2014**, *4*, 24710.
[142] Y. Xu, M. Mazzawi, K. Chen, L. Sun, P. L. Dubin, *Biomacromolecules* **2011**, *12*, 1512.
[143] P. M. Biesheuvel, M. A. Cohen Stuart, *Langmuir* **2004**, *20*, 2785.
[144] Y. Li, Q. Huang, *J. Phys. Chem. B* **2013**, *117*, 2615.
[145] E. Seyrek, P. L. Dubin, C. Tribet, E. A. Gamble, *Biomacromolecules* **2003**, *4*, 273.
[146] J. M. Park, B. B. Muhoberac, P. L. Dubin, J. Xia, *Macromolecules* **1992**, *25*, 290.
[147] J. Xia, P. L. Dubin, Y. Kim, B. B. Muhoberac, V. J. Klimkowski, *J. Phys. Chem.* **1993**, *97*, 4528.
[148] R. de Vries, F. Weinbreck, C. G. de Kruif, *J Chem Phys* **2003**, *118*, 4649.
[149] N. Pippa, M. Karayianni, S. Pispas, C. Demetzos, *Int. J. Pharm.* **2015**, *491*, 136.
[150] T. Chida, Y. Miura, H. Cabral, T. Nomoto, K. Kataoka, N. Nishiyama, *J. Controlled Release* **2018**, *292*, 130.
[151] A. Harada, K. Kataoka, *J. Controlled Release* **2001**, *72*, 85.
[152] C. P. Brangwynne, T. J. Mitchison, A. A. Hyman, *PNAS* **2011**, *108*, 4334.
[153] A. A. Hyman, K. Simons, *Science* **2012**, *337*, 1047.
[154] S. C. Weber, C. P. Brangwynne, *Cell* **2012**, *149*, 1188.
[155] S. C. Weber, *Curr Opin Cell Biol* **2017**, *46*, 62.
[156] A. A. Hyman, C. A. Weber, F. Jülicher, *Annu. Rev. Cell Dev. Biol.* **2014**, *30*, 39.
[157] C. P. Brangwynne, P. Tompa, R. V. Pappu, *Nat Phys* **2015**, *11*, 899.
[158] L. Zhu, C. P. Brangwynne, *Curr Opin Cell Biol* **2015**, *34*, 23.
[159] C. A. Bayas, J. Wang, M. K. Lee, J. M. Schrader, L. Shapiro, W. E. Moerner, *PNAS* **2018**, *115*, E3712.
[160] J. N. Werner, E. Y. Chen, J. M. Guberman, A. R. Zippilli, J. J. Irgon, Z. Gitai, *PNAS* **2009**, *106*, 7858.
[161] A. Jain, S. K. Singh, S. K. Arya, S. C. Kundu, S. Kapoor, *ACS Biomater. Sci. Eng.* **2018**, *4*, 3939.
[162] Z. Ou, M. Muthukumar, *J Chem Phys* **2006**, *124*, 154902.
[163] S. Saurabh, P. K. Sahoo, *Aquacult Res* **2008**, *39*, 223.
[164] S. A. Ragland, A. K. Criss, *PLoS Pathog* **2017**, *13*, e1006512.
[165] H. R. Ibrahim, T. Matsuzaki, T. Aoki, *FEBS Lett.* **2001**, *506*, 27.
[166] S. Lindhoud, R. de Vries, R. Schweins, M. A. Cohen Stuart, W. Norde, *Soft Matter* **2009**, *5*, 242.
[167] S. Lindhoud, R. de Vries, W. Norde, M. A. Cohen Stuart, *Biomacromolecules* **2007**, *8*, 2219.
[168] S. Lindhoud, L. Voorhaar, R. de Vries, R. Schweins, M. A. Cohen Stuart, W. Norde, *Langmuir* **2009**, *25*, 11425.
[169] G. Gao, Y. Yan, S. Pispas, P. Yao, *Macromol. Biosci.* **2010**, *10*, 139.
[170] N. R. Johnson, T. Ambe, Y. Wang, *Acta Biomater.* **2014**, *10*, 40.
[171] B. J. S. C. Olson, J. Markwell, *Assays for Determination of Protein Concentration.*, John Wiley & Sons, Inc., Hoboken, NJ, USA, **2007**.
[172] Y. A. Antonov, I. L. Zhuravleva, R. Cardinaels, P. Moldenaers, *Food Hydrocolloids* **2018**, *74*, 227.
[173] M. H. Simonian, *Curr Protoc Cell Biol* **2002**, *15*, A.3B.1.
[174] A. R. Rudke, S. A. Heleno, I. P. Fernandes, M. A. Prieto, O. H. Gonçalves, A. E. Rodrigues, I. C. F. R. Ferreira, M. F. Barreiro, *LWT - Food Science and Technology* **2019**, *103*, 228.
[175] M.-F. Li, L. Chen, M.-Z. Xu, J.-L. Zhang, Q. Wang, Q.-Z. Zeng, X.-C. Wei, Y. Yuan, *Int. J. Biol.*

Macromol. **2018**, *116*, 1232.
[176] J. J. Water, M. M. Schack, A. Velazquez-Campoy, M. J. Maltesen, M. van de Weert, L. Jorgensen, **2014**, *88*, 325.
[177] F. H. Niesen, H. Berglund, M. Vedadi, *Nat Protoc* **2007**, *2*, 2212.
[178] R. J. Johnson, C. J. Savas, Z. Kartje, G. C. Hoops, *J. Chem. Educ.* **2014**, *91*, 1077.
[179] A. C. Miklos, M. Sarkar, Y. Wang, G. J. Pielak, *J Am Chem Soc* **2011**, *133*, 7116.
[180] S. P. Santero, F. Favretto, S. Zanzoni, R. Chignola, M. Assfalg, M. D'Onofrio, *Arch. Biochem. Biophys.* **2016**, *606*, 99.
[181] D. Houde, S. A. Berkowitz, J. R. Engen, *J. Pharm. Sci.* **2011**, *100*, 2071.
[182] Y. Hamuro, S. J. Coales, M. R. Southern, J. F. Nemeth-Cawley, D. D. Stranz, P. R. Griffin, *J Biomol Tech* **2003**, *14*, 171.
[183] I. B. Durowoju, K. S. Bhandal, J. Hu, B. Carpick, M. Kirkitadze, *JoVE* **2017**, 1.
[184] C. M. Johnson, *Arch. Biochem. Biophys.* **2013**, *531*, 100.
[185] O. N. Ivinova, V. A. Izumrudov, V. I. Muronetz, I. Y. Galaev, B. Mattiasson, *Macromol. Biosci.* **2003**, *3*, 210.
[186] E. Sedlák, D. Fedunová, V. Veselá, D. Sedláková, M. Antalík, *Biomacromolecules* **2009**, *10*, 2533.
[187] S. V. Stogov, V. A. Izumrudov, V. I. Muronetz, *Biochemistry (Moscow)* **2010**, *75*, 437.
[188] N. Greenfield, G. D. Fasman, *Biochemistry* **1969**, *8*, 4108.
[189] W. C. Johnson Jr, *Ann Rev Biophys Biophys Chem* **1988**, *17*, 145.
[190] Z. Peng, S. Li, X. Han, A. O. Al-Youbi, A. S. Bashammakh, M. S. El-Shahawi, R. M. Leblanc, *Anal. Chim. Acta* **2016**, *937*, 113.
[191] N. Devi, M. Sarmah, B. Khatun, T. K. Maji, *Adv. Colloid Interface Sci.* **2016**, In Press.
[192] L. Mazzaferro, J. D. Breccia, M. M. Andersson, B. Hitzmann, R. Hatti-Kaul, *Int. J. Biol. Macromol.* **2010**, *47*, 15.
[193] R. Shaddel, J. Hesari, S. Azadmard-Damirchi, H. Hamishehkar, B. Fathi-Achachlouei, Q. Huang, *Int. J. Biol. Macromol.* **2018**, *107*, 1800.
[194] D. Sueyoshi, Y. Anraku, T. Komatsu, Y. Urano, K. Kataoka, *Biomacromolecules* **2017**, *18*, 1189.
[195] L. Y. Filatova, D. M. Donovan, S. C. Becker, D. N. Lebedev, A. D. Priyma, H. V. Koudriachova, A. V. Kabanov, N. L. Klyachko, *Biochimie* **2013**, *95*, 1689.
[196] B. S. Schuster, E. H. Reed, R. Parthasarathy, C. N. Jahnke, R. M. Caldwell, J. G. Bermudez, H. Ramage, M. C. Good, D. A. Hammer, *Nat Commun* **2018**, *9*, eaaf4382.
[197] S. Koga, D. S. Williams, A. W. Perriman, S. Mann, *Nat Chem* **2011**, *3*, 720.
[198] N. Martin, M. Li, S. Mann, *Langmuir* **2016**, *32*, 5881.
[199] J. Berry, C. P. Brangwynne, M. Haataja, *Rep. Prog. Phys.* **2018**, *81*, 046601.
[200] V. N. Uversky, *Adv. Colloid Interface Sci.* **2017**, *239*, 97.
[201] G. M. Tavares, T. Croguennec, P. Hamon, A. F. Carvalho, S. Bouhallab, *Food Hydrocolloids* **2015**, *48*, 238.
[202] Y. Xu, M. Liu, M. Faisal, Y. Si, Y. Guo, *Adv. Colloid Interface Sci.* **2017**, *239*, 158.